Supporting Information

Non-Conjugated Electrochromic Supercapacitors with Atom-Economic Arylamine-Based AB_2-Polyamide

Yu-Jen Shao, [a] *Yi-Ju Cho,* [a] *Hou-Lin Li,* [a] *Chien-Chieh Hu,*[b]* *Guey-Sheng Liou* [a]*

[a] Institute of Polymer Science and Engineering, National Taiwan University, No. 1, Sec. 4, Roosevelt Rd., Taipei 10617, Taiwan. E-mail: gsliou@ntu.edu.tw

[b] Graduate Institute of Applied Science and Technology, National Taiwan University of Science and Technology, Taipei 106335, Taiwan. E-mail: cchu@mail.ntust.edu.tw

Keywords: electrochromism, switching capability enhancement, AB_2-type hyperbranched polyamide, arylamine derivatives, intrinsic microporosity

List of Contents for Supplementary Information:

Materials

The 4-methoxyl-4′-nitrodiphenylamine (**1**) (m. p. =151–153 ℃) and 4-cyano-4′-methoxyl-4″-nitrotriphenylamine (**2**) (m. p. =171–173 ℃) were synthesized by nucleophilic substitution, according to a previously reported literature.[1] 4-Carboxy-4′,4″dimethoxytriphenylamine (**TPA**) (m. p. = 203–205 ºC) was prepared by Ullmann and hydrolysis reactions.[2] 4-Fluoronitrobenzene (Alfa Aesar), *p*-anisidine (ACROS), triethylamine (TEA; ACROS), 4-fluorobenzonitrile (TCI), potassium carbonate (Alfa Aesar), cesium fluoride (CsF; ACROS), sodium *tert*-butoxide (NaO*t*Bu, Alfa Aesar), 4-aminobenzonitrile (Matrix), copper powder (Acros), 18-crown-6-ether (TCI), 4-iodoanisole (ACROS), hydrazine monohydrate (Alfa Aesar), 10% Pd/C (ACROS), benzoic acid (**BA**, SHOWA), dimethyl sulfoxide (DMSO; ECHO), triphenyl phosphite (TPP; ACROS), *o*-dichlorobenzene (TEDIA), *N*,*N*-dimethylformamide (DMF; ACROS), tetrahydrofuran (THF; ECHO) were used as received without further purification. *N*,*N*-dimethylacetamide (DMAc), *N*-methyl-2-pyrrolidinone (NMP; TEDIA), and pyridine (Py; ECHO) underwent purification through distillation under reduced pressure with calcium hydride. Additionally, commercially acquired anhydrous calcium chloride ($CaCl_2$) was subjected to drying under vacuum conditions at 180 ℃ for 8 hours. The supporting electrolyte, tetrabutylammonium tetrafluoroborate ($TBABF_4$), was prepared by gradually adding an aqueous solution of tetrabutylammonium bromide (TBAB; TCI) into a stirred solution of saturated sodium tetrafluoroborate ($NaBF_4$; ACROS). The resulting white residue was recrystallized using an ethanol/water solution and dried under vacuum before utilization.

Measurement

Inherent viscosities of the polyamides were measured with Glass capillary viscometers with a concentration of 0.5 g/dL NMP at 30 ℃ in the Tamson TV2000 viscometer bath. Molecular weights and polydispersity index (PDI) were reported by gel permeation chromatographic (GPC) analysis through a Waters chromatography unit interfaced with a Waters 2410 refractive index detector. Two Shodex GPC KD-803 and GPC KD-804 were connected in the system with LiCl salt in NMP (20 mM)

as the eluent at a flow rate of 0.35 mL/min at 40 ℃ and calibrated using polystyrene standards. Fourier transform infrared (FT-IR) spectra were conducted using a PerkinElmer Spectrum. The ^{1}H-NMR and ^{13}C-NMR spectra were measured on a Bruker AVIII HD-600 (600 MHz) or Bruker AVIII-500 (500 MHz), using dimethyl sulfoxide (DMSO-d_6) as solvent and tetramethylsilane (TMS; δ = 0 ppm) as internal standard. Mass spectra were measured with Thermo Scientific™ Q Exactive™ Plus Hybrid Quadrupole-Orbitrap™ Mass Spectrometer operating in electrospray ionization (ESI) mode. Thermal stability was used to conduct by Thermogravimetric analysis (TGA, TA instrument Q50) with 3-8 mg of the prepared samples at a heating rate of 20 ℃/min under nitrogen and air systems (flowing rate: 60 cm^3/min) and differential scanning calorimeter (DSC) with TA instruments Q-20. Transparency and colour coordination of the polymer films were determined by JASCO V650 and HITACHI U4100 UV-vis spectrophotometer, and the absorbance spectrum of switching time was recorded on Agilent UV-vis spectrophotometer. Electrochemical properties, including cyclic voltammetry (CV), differential pulse voltammetry (DPV), and electrochemical impedance spectroscopy (EIS), were conducted through CH Instruments 6122E Electrochemical Analyzer. Electrochemical Analyzer used a three-electrode system containing a platinum counter electrode, a polymer film coated on ITO glass (0.6 cm × 3 cm) as working electrode, and an Ag/AgCl reference electrode in 30 mL anhydrous acetonitrile with 0.1 M $TBABF_4$ as supporting electrolyte under the air atmosphere. The testing frequency of EIS was from 1M Hz to 0.1 Hz. The scanning rate of CV was set from 10 mV/s to 100 mV/s to investigate the diffusivities of each polymer. Wide-angle X-ray diffraction (WXRD) was run on BRUKER, D8 DISCOVER SSS Multi-Function High Power X-Ray diffractometer under CuKα radiation (wavelength: 1.54 Å). The specific surface area was determined by analyzing the results of the BET instrument, the Micromeritics ASAP 2060.

Preparation of the polymeric films

The thick film was prepared by dissolving 50 mg polymer in 3 mL NMP. The solution was filtrated through a syringe filter and drop-casting on a 75 mm × 26 mm glass slide, placed in a vacuum oven, and removed most of the solvent at room temperature. The oven temperature was raised to 180 ℃ for 12 hours to dry the film completely. The films obtained had a thickness of approximately 25 ± 5 μm and were utilized for various analyses, including solubility tests, thermal analysis, WXRD, and BET measurements. The polymeric electrodes were made by drop-casting on the 30 mm × 25 mm ITO glass using a 300 μL solution containing 2 mg of the produced polymer in 1 mL DMF to conduct the electrochemical tests. Most of the solvent was removed in the vacuum oven at 60 ℃ after being dropped on the ITO glass. To ensure all the solvent was eliminated, the temperature was increased to 120 ℃ for 2 h and 180 ℃ for 8 h in vacuo. The polymer film-coated ITO glass was cut to the required size for each measurement.

Fabrication of the electrochromic devices (ECDs)

Two 30 mm x 25 mm ITO-coated glass pieces were initially prepared as electrodes, with one glass coated with electroactive polyamides (300 ± 50 nm thickness) to fabricate the ECDs. Subsequently, a thermoset adhesive frame (20 mm × 20 mm) with a 5 mm width break was dispensed using an auto-dispenser. The two glasses were then adhered together to form an empty device, with the gap distance regulated by a 120 μm spacer in the adhesive. The adhesive was cured in an oven at 150 ℃ for 10 h. Finally, a liquid-type electrolyte was introduced into the device through the 5 mm width break under a vacuum, and the break was sealed with UV gel. The liquid-type electrolyte was composed of 165 mg $TBABF_4$ at a concentration of 0.1 M, 40 mg of HV at a concentration of 0.015 M, and 5 mL of propylene carbonate (PC). The total volume of the injected electrolyte was approximately 48 μL.

Experimental methods

Synthesis of AB_2–type Monomer (TPPA-AB_2)

4-Methoxy-4′-nitrodiphenylamine (1) and **4-cyano-4′-methoxy-4″-nitrotriphenylamine (2)**

According to well-known compound,[1] compound **1** (m.p. =151—153 ºC; lit.[1] m.p. = 153—154 ºC) and compound **2** (m.p. =171—173 ºC; lit.[1] m.p. = 134-141 ºC) were prepared by the triethylamine-mediated aromatic nucleophilic substitution reaction of 4-fluoronitrobenzene and *p*-anisidine followed by the potassium carbonate-mediated nucleophilic substitution reaction of 4-fluorobenzonitrile.

4-Amino-4′-methoxy-4″-nitrotriphenylamine (3)

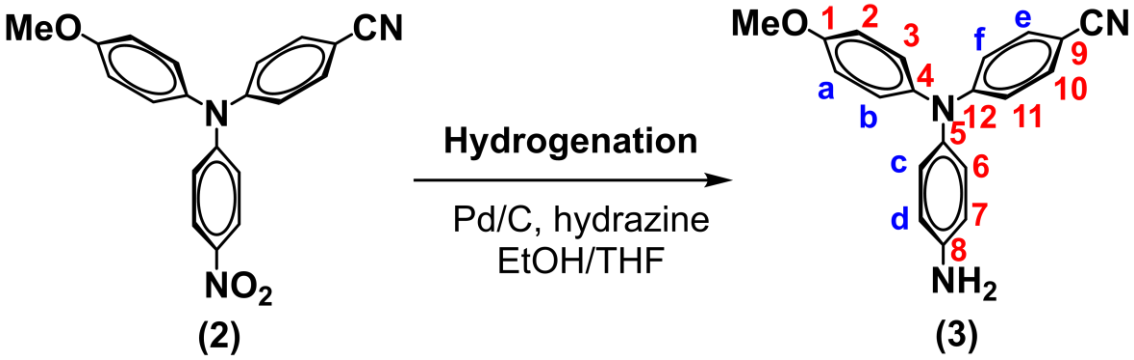

In a 100 mL three-neck round-bottomed flask equipped with a stirring bar under nitrogen atmosphere, 6.91 g (20 mmol) of compound **2** and 0.2 g of 10% Pd/C were dissolved in 20 mL of ethanol and 30 mL of tetrahydrofuran (THF). The solution was heated to reflux, and 3 mL of hydrazine monohydrate was added slowly. After the solution was stirred at reflux temperature for 12 h, Celite® 545 particles filtered the solution to remove Pd/C, and the filtrate was cooled to precipitate. The product was collected by filtration and dried in vacuo at 80 °C for 10 h to give 6.03 g (96% in yield) of pale-yellow crystal with the m.p. of 151–153 °C by DSC at a scan rate of 10 °C/min. FT-IR (KBr) spectrum: 3433, 3350 cm^{-1} (primary N–H stretch), 2215 cm^{-1} (–C≡N stretch). ^{1}H-NMR (600 MHz, DMSO-d_6) δ: 3.75 (s, 3H, –OMe), 5.21 (s, 2H, -NH_2), 6.58 (d, 2H, H_f), 6.61 (d, 2H, H_d), 6.93 (d, 2H, H_c), 6.97 (d, 2H, H_a), 7.18 (d, 2H, H_b), 7.47 (d, 2H, H_e). ^{13}C-NMR (150 MHz, DMSO-d_6) δ: 55.29 (–OMe), 97.91 (C_9), 114.88 (C_{11}), 114.91 (C_7), 115.18 (C_2), 120.05 (–C≡N), 128.20 (C_3), 128.38 (C_6), 133.10 (C_5), 133.15

(C_{10}), 138.07 (C_4), 147.39(C_8), 152.60(C_{12}), 157.05 (C_1). HRMS (m/z), [M + H^+] calculated: 316.1444, found:316.1441.

***N*,*N*-Bis(4-nitrophenyl)-*N*′(4-cyanophenyl)-*N*′-(4′-methoxyphenyl)-1,4-phenylenediamine (4)**

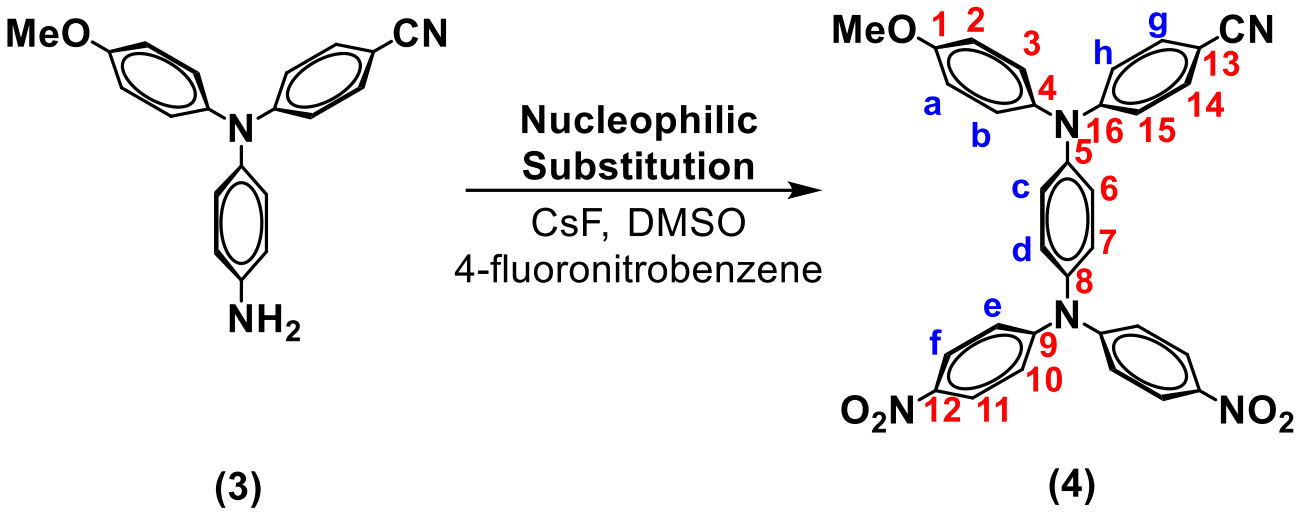

(3) **(4)**

A mixture of 4.86 g (30 mmol) of dry CsF, 3.80 g (12 mmol) of mono-amine compound **3,** and 4-fluoronitrobenzene with 3.95 g (28 mmol) was added in sequence in 15 mL of DMSO. The mixture was stirred and heated at 150 ℃ for 48 h under a nitrogen atmosphere. The mixture was poured into 500 mL of stirred methanol/water. The precipitated red powder was redissolved in DMF, reprecipitated in MeOH, and filtrated to obtain the dinitro compound. The powder was dried in vacuo at 100 ℃ for 10 h to give 5.56 g (83% in yield) with the m.p. of 249–250 ℃ by DSC at a scan rate of 10 ℃/min. FT-IR (KBr) spectrum: 2220 cm^{-1} (–C≡N stretch),1590 and 1310 cm^{-1} (symmetric and asymmetric –NO_2 stretch). ^{1}H-NMR (600 MHz, DMSO-d_6) δ: 3.78 (s, 3H, –OMe), 6.90 (d, 2H, H_h), 7.05 (d, 2H, H_a), 7.23 (d, 2H, H_b), 7.24 (m, 4H, H_c + H_d), 7.26 (d, 4H, H_e), 7.62 (d, 2H, H_g), 8.20 (d, 4H, H_f). ^{13}C-NMR (150 MHz, DMSO-d_6) δ: 55.36 (–OMe), 100.92 (C_{13}), 115.62 (C_2), 118.17 (C_{15}), 119.53 (-C≡N), 122.49 (C_{10}), 125.60 (C_{11}), 126.72 (C_6), 128.60 (C_7), 129.00 (C_3), 133.44 (C_{14}), 137.52 (C_8), 140.51 (C_4), 142.07 (C_{12}), 143.90 (C_5), 151.33 (C_{16}), 151.52 (C_9), 157.61 (C_1). HRMS (m/z), [M + H^+] calculated: 558.1772, found: 558.1760.

***N*,*N*-Bis(4-aminophenyl)-*N*′-(4-carboxyphenyl)-*N*′-(4′-methoxyphenyl)-1,4-phenylenediamine (TPPA-AB$_2$)**

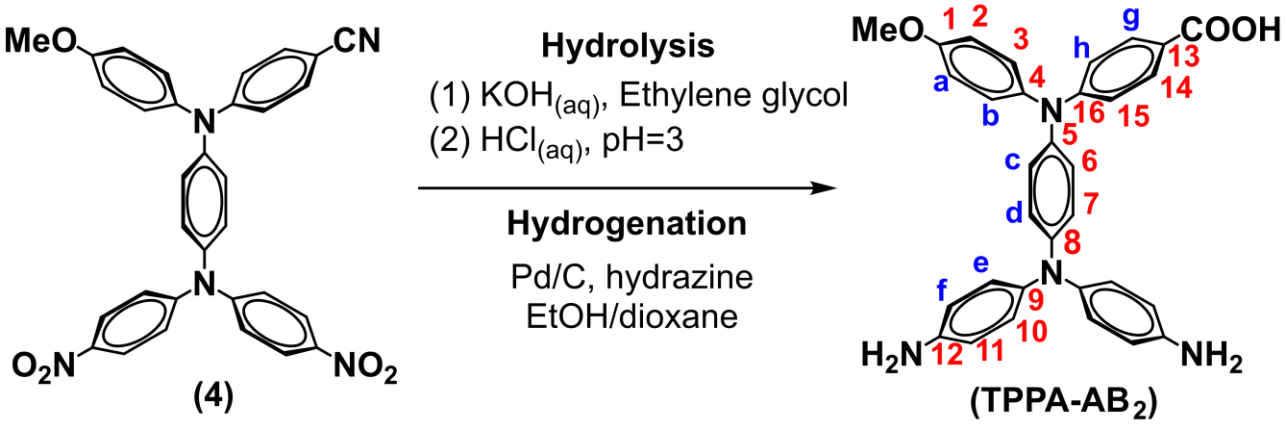

A mixture of 7.85g of potassium hydroxide and 5.78 g (10 mmol) of compound **4** in 20 mL of ethylene glycol and 10 mL of distilled water was stirred at 210 ℃ until no further ammonia was generated. The time taken to reach the stage was about 5-6 days. The solution was cooled, and the pH value was adjusted by hydrochloric acid (6 M HCl) to near 3. The black-red precipitate formed was collected by filtration, washed thoroughly with water and methanol, and then dried at 100 ℃ in vacuo for 10 h to give dark-red powder. Following, in a 100 mL three-neck round-bottomed flask equipped with a stirring bar under a nitrogen atmosphere, 0.58 g (1 mmol) of dark-red powder and 0.05 g of 10% Pd/C were suspended in 10 mL of ethanol and dioxane, respectively. Hydrazine monohydrate was added slowly to the mixture and heated to the reflux temperature. After the solution was stirred for 24 hours, it was filtered by Celite® 545 to remove Pd/C, and the filtrate was concentrated under reduced pressure. Then, the filtrate was poured into water to precipitate. The product was collected by filtration and dried in vacuo at 100 ℃ for 15 h to give 0.50 g (92% in yield) of pale-yellow crystal, and the m.p. was non-detected up to 300 ℃ by DSC at a scan rate of 10 ℃ /min. FT-IR (KBr): 3440, 3355 cm^{-1} (–NH_2 stretch), 3400-2700 cm^{-1} (–OH stretch), and 1680 cm^{-1} (C=O stretch). ^{1}H-NMR (600 MHz, DMSO-d_6) δ: 3.75 (s, 3H, –OMe), 6.54 (d, 4H, H_f), 6.58 (d, 2H, H_a), 6.62 (d, 2H, H_h), 6.84 (d, 4H, H_e), 6.92 (d, 2H, H_b), 6.94 (d, 2H, H_d), 7.12 (d, 2H, H_c), 7.67 (d, 2H, H_g). ^{13}C-NMR (150 MHz, DMSO-d_6) δ: 55.22 (–OMe), 114.73 (C_{11}), 115.09 (C_3), 115.20 (C_{15}), 117.05 (C_2), 118.86 (C_{13}), 127.45

(C_{10}), 127.45 (C_7), 127.95 (C_6), 130.68 (C_{14}), 135.59 (C_9), 138.66 (C_4), 144.00 (C_8),145.72 (C_{12}), 147.33 (C_5), 152.37 (C_{16}), 156.64 (C_1), 167.09 (C=O). HRMS (m/z), [M + H^+] calculated: 517.2234, found: 517.2234.

Synthesis of AB-type Monomer (TPPA-AB)

***N*-(4-Cyanophenyl)-*N*-(4′-methoxyphenyl)-*N*′-(4-nitrophenyl)-1,4-phenylenediamine (5)**

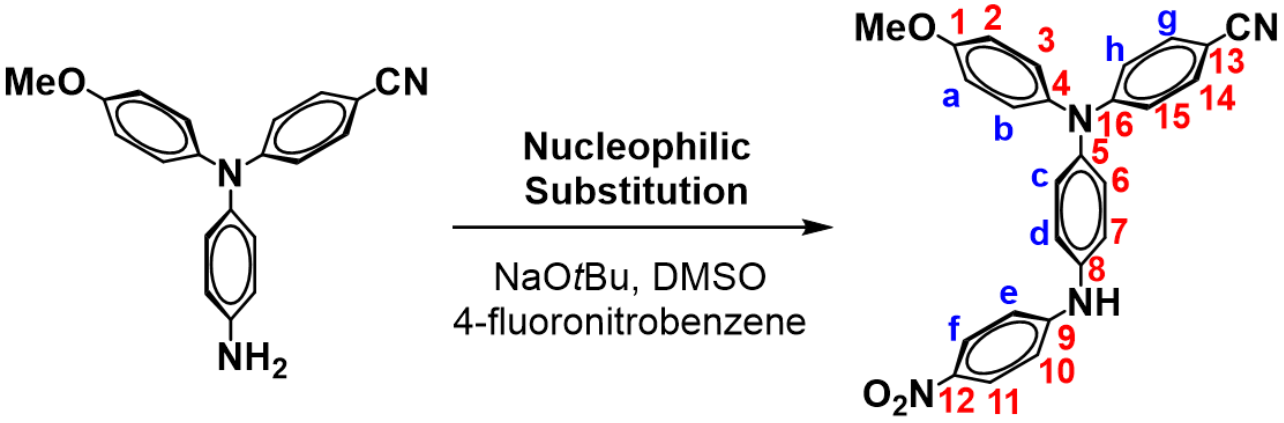

(3) **(5)**

In a 250 mL three-neck round-bottomed flask equipped with a stirring bar under a nitrogen atmosphere, 4.71 g of compound **3** and 1.52 g of NaO*t*Bu were dissolved in 10 mL of DMSO. The 4-fluoronitrobenzene (1.56 mL) was diluted in 40 mL of DMSO and added dropwise slowly. The mixture was stirred at room temperature for 4 h under a nitrogen atmosphere and then precipitated into 700 mL of cold water. The product was filtered, recrystallized from ethanol, and dried in vacuo at 80 ℃ for 10 h to give 4.52 g of red-orange powder (69% in yield) with the m.p. of 217–219 ℃ by DSC at a scan rate of 10 ℃/min. FT-IR (KBr): 3315 cm^{-1} (secondary N-H stretch), 2215 cm^{-1} (C≡N stretch), 1590 and 1310 cm^{-1} (symmetric and asymmetric –NO_2 stretch). ^{1}H-NMR (600 MHz, DMSO-d_6) δ: 3.77 (s, 3H, –OMe), 6.73 (d, 2H, H_h), 7.00 (d, 2H, H_a), 7.07 (d, 2H, H_e), 7.19 (m, 4H, H_{b+d}), 7.27 (d, 2H, H_c), 7.54 (d, 2H, H_g), 8.08 (d, 2H, H_f), 9.34 (-NH). ^{13}C-NMR (150 MHz, DMSO-d_6) δ: 55.29 (–OMe), 99.58 (C_{13}), 113.50 (C_{10}), 115.40 (C_2), 116.51(C_{15}), 119.66 (–CN), 121.89 (C_6), 126.08 (C_{11}), 127.44 (C_3), 128.59 (C_7), 133.29 (C_{14}), 137.53 (C_8), 137.67 (C_4), 138.01 (C_5), 140.24 (C_{12}), 150.43 (C_{16}), 151.74 (C_9), 157.35 (C_1). HRMS (m/z), [M + H^+] calculated: 437.1608, found: 437.1607.

***N*,*N*′-Bis(4-methoxyphenyl)-*N*-(4-cyanophenyl)-*N*′-(4-nitrophenyl)-1,4-phenylenediamine (6)**

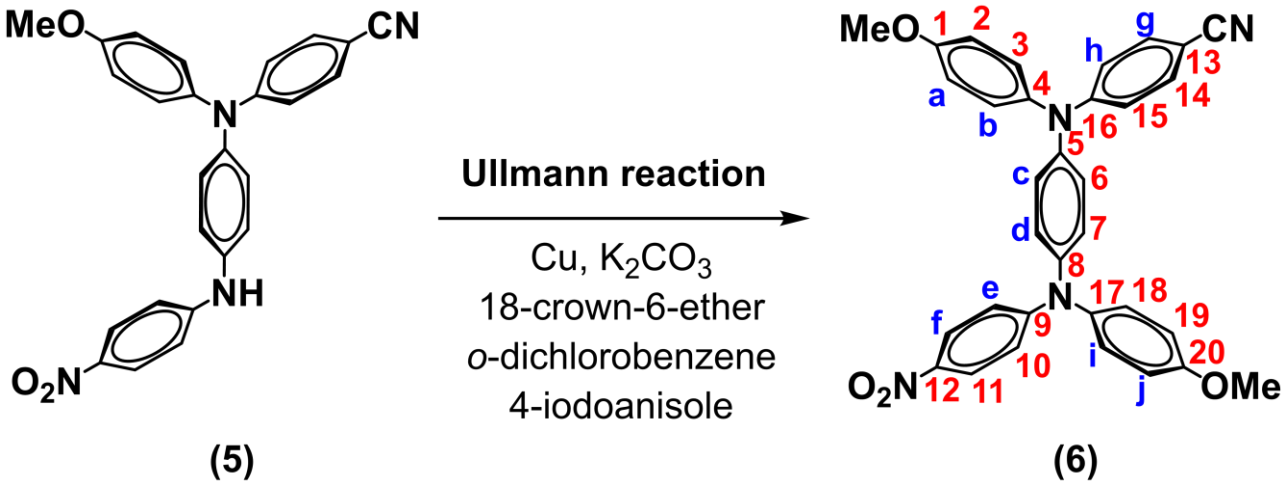

(5) **(6)**

Ullmann reaction was used to synthesize the new compound **7**. In a 100 mL three-neck round-bottomed flask equipped with a stirring bar under nitrogen atmosphere, 0.76 g of copper powder, 2.81 g of 4-iodoanisole, 3.41 g of compound **6**, and 1.66 g of powdered anhydrous potassium carbonate were added in sequence with 0.79 g of 18-crown-6-ether and dissolved in 20 mL of *o*-dichlorobenzene. After the reaction mixture was refluxed for 12 h, the mixture was filtered by Celite® 545 and further purified by column chromatography with an eluent of dichloromethane and dried in vacuo at 80 °C for 10 h to obtain 3.16 g of dark-red powder (75 % in yield) with a m.p. of 218–220 °C by DSC at a scan rate of 10 °C/min. FT-IR (KBr) spectrum: 2215 cm^{-1} (C≡N stretch), 1590 and 1310 cm^{-1} (symmetric and asymmetric –NO_2 stretch). ^{1}H-NMR (600 MHz, DMSO-d_6) δ: 3.77 (s, 3H, –OMe), 3.78 (s, 3H, –OMe), 6.76 (d, 2H, H_e), 6.80 (d, 2H, H_h), 7.01 (m, 4H, H_j+H_a), 7.19 (m, 8H, H_i+H_c+H_b+H_d), 7.57 (d, 2H, H_g), 8.04 (d, 2H, H_f). ^{13}C-NMR (150 MHz, DMSO-d_6) δ: 55.83 (–OMe), 55.86 (–OMe), 100.88 (C_{13}), 116.06 (C_2), 116.10 (C_{19}), 116.31 (C_{10}), 118.00 (C_{15}), 120.07 (–CN), 126.13 (C_{11}), 127.42 (C_7), 128.17 (C_6), 129.42 (C_{18+3}), 133.89 (C_{14}), 137.79 (C_4), 138.06 (C_{17}), 138.99 (C_5), 142.00 (C_8), 143.29 (C_{12}), 151.98 (C_{16}), 154.12 (C_9), 158.04 (C_1), 158.30 (C_{20}). HRMS (m/z), [M + H^+] calculated: 543.2027, found: 543.2024.

***N*,*N*′-Bis(4-methoxyphenyl)-*N*-(4-carboxyphenyl)-*N*′-(4-aminophenyl)-1,4-phenylenediamine (TPPA-AB)**

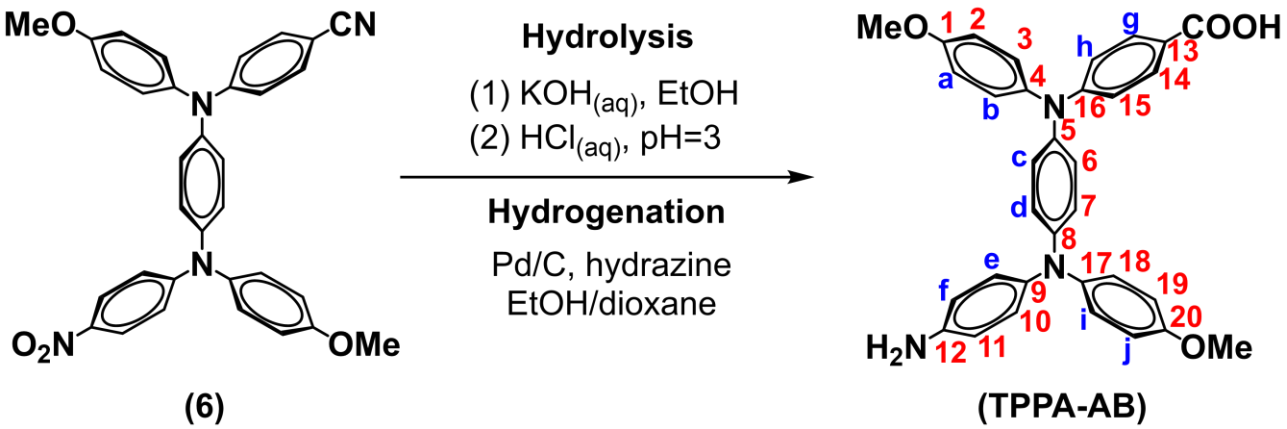

(6) (TPPA-AB)

A mixture of 4.32 g of potassium hydroxide and 3.02 g (5.5 mmol) of compound **6** in 20 ml of ethanol and 10 ml of distilled water was stirred at 100 ℃ until no further ammonia was generated. The time taken to reach the stage was about 4-5 days. The solution was cooled, and the pH value was adjusted by hydrochloric acid (6 M HCl) to near 3. The dark-red precipitate formed was collected by filtration, washed thoroughly with water and methanol, and then dried at 100 ℃ in vacuo for 10 h to give 3.21 g dark-red powder. Then, 1.77 g (3 mmol) of dark-red powder and 0.14 g of 10% Pd/C were added in 10 mL of ethanol in a 100 mL three-neck round-bottomed flask equipped with a stirring bar under a nitrogen atmosphere. Hydrazine monohydrate was added slowly to the mixture and heated to the reflux temperature. After the solution was stirred for hours, it was filtered by Celite® 545 to remove Pd/C, and the filtrate was concentrated under reduced pressure. The product was collected by filtration and dried in vacuo at 80 ℃ to give 1.26 g (72% in yield) of pale-yellow crystal, and the m.p. was non-detected before 300 ℃ by DSC at a scan rate of 10 ℃/min. FT-IR (KBr): 3445, 3355 cm^{-1} (NH_2 stretch), 3600-2700 cm^{-1} (–OH stretch), and 1670 cm^{-1} (C=O stretch). ^1H NMR (600 MHz, DMSO-d_6) δ: 3.71 (s, 3H, –OMe), 3.75 (s, 3H, –OMe), 6.55 (d, 2H, H_f), 6.65 (m, 4H, H_d+H_h), 6.70 (m, 4H, H_j+H_e), 6.88 (m, 4H, H_a+H_c), 7.02 (d, 2H, H_i), 7.12 (d, 2H, H_b), 7.69 (d, 2H, H_g). ^{13}C NMR (150 MHz, DMSO-d_6) δ: 55.17 (–OMe), 55.23 (–OMe), 114.74 (C_{11}), 114.89 (C_{19}), 115.13 (C_2), 115.66 (C_{15}), 118.90 (C_7), 120.57 (C_{13}), 126.09 (C_{18}), 127.25 (C_6), 127.66 (C_{10}), 127.98 (C_3), 130.68 (C_{14}), 135.31 (C_{12}), 137.00

(C_{17}), 138.67 (C_4), 140.34 (C_8), 146.01 (C_5), 146.33 (C_9), 152.09 (C_{16}), 155.33 (C_1), 156.67 (C_{20}), 167.17 (C=O). HRMS (m/z), [M + H^+] calculated: 532.2231, found: 532.2233.

Synthesis of Polyamides

This study synthesized three polyamides, with **TPPA-AB** and **TPPA-AB$_2$** prepared via direct polycondensation to obtain linear polyamide (**LPA**) and hyperbranched polyamide (HPA). Additionally, the HPA polymer solution undergoes the end-capped reaction with the end-capped agents of 4-carboxy-4′,4″-dimethoxytriphenylamine, and benzoic acid to produce **HPA-TPA** and **HPA-B**, respectively. Following are descriptions of their synthesis pathways, and **Tables S1** and **S2** summarize the resulting molecular weights and solubility characteristics.

Preparation of AB$_2$ Hyperbranched Polyamide

According to the previously reported literature.[3] In a flask, 0.76 g (1.5 mmol) of the compound (**TPPA-AB$_2$**) was dissolved in 2 mL of NMP. Subsequently, 0.2 g of $CaCl_2$, 0.6 mL of pyridine, and 0.787 mL of TPP were added to the flask. After the mixture was heated to 100 °C and stirred under a nitrogen atmosphere for 3 h, the polymer solution was diluted to 10 wt%. Then, 4 mL of the polymer solution was transferred to another flask, and the end-capping agents (benzoic acid and 4-carboxy-4′,4″-dimethoxytriphenylamine) were respectively added. The mixture was stirred at 100 °C for 6 h under a nitrogen atmosphere. After that, the end-capped hyperbranched polymer solution was slowly poured into 400 mL of a stirred methanol/water mixture (1:1, v/v), forming a flaky precipitate. The precipitate was collected by filtration, and Soxhlet extraction with hot water and methanol was used for one day each to purify. The yield was 96% for **HPA-TPA** and 95% for **HPA-B**.

Preparation of AB Linear Polyamide

In a flask, 0.13 g (0.25 mmol) of the compound (**TPPA-AB**) was dissolved in 0.1 mL of NMP. Subsequently, 0.014 g of $CaCl_2$, 0.175 mL of pyridine, and 0.098 mL of TPP were added to the flask. After the mixture was heated to 100 °C and stirred under a nitrogen atmosphere for 3 hours, the polymer solution was slowly poured into 400 mL of a stirred methanol/water mixture (1:1, v/v), forming a flaky precipitate. The precipitate was collected by thorough filtration, and Soxhlet extraction

with hot water and methanol was used for one day each to purify. The yield was 82%. FT-IR(KBr): 3315 cm^{-1} (-NH stretch), and 1655 cm^{-1} (C=O stretch).

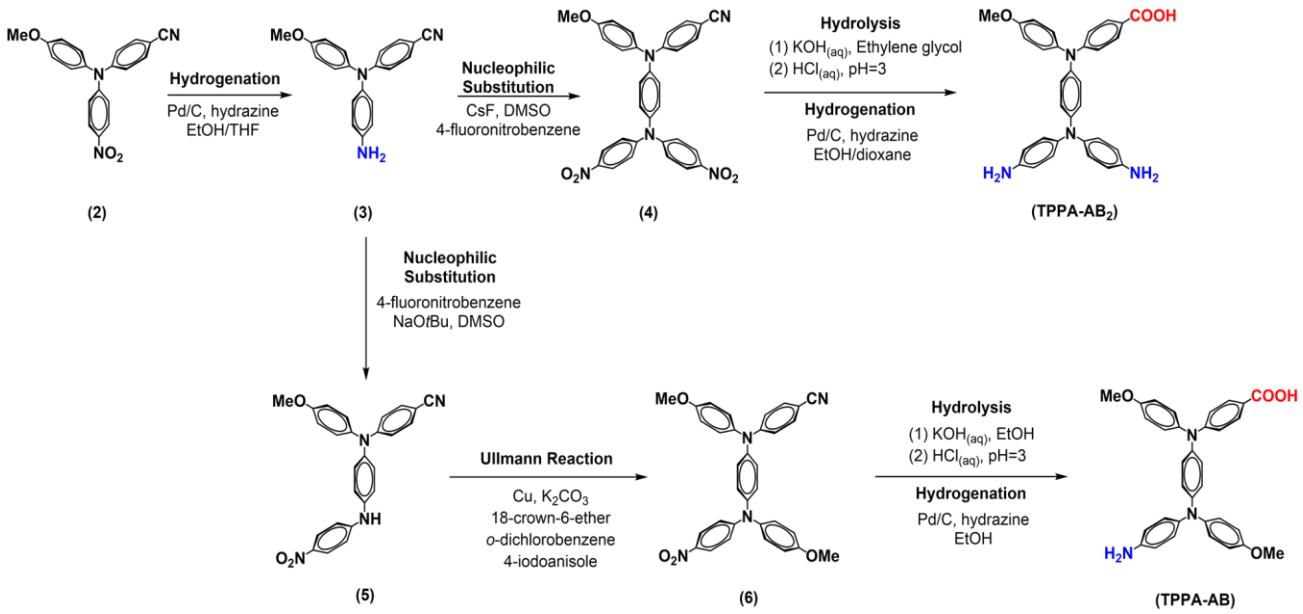

Scheme S1. Synthetic routes of monomers **TPPA-AB2** and **TPPA-AB**.

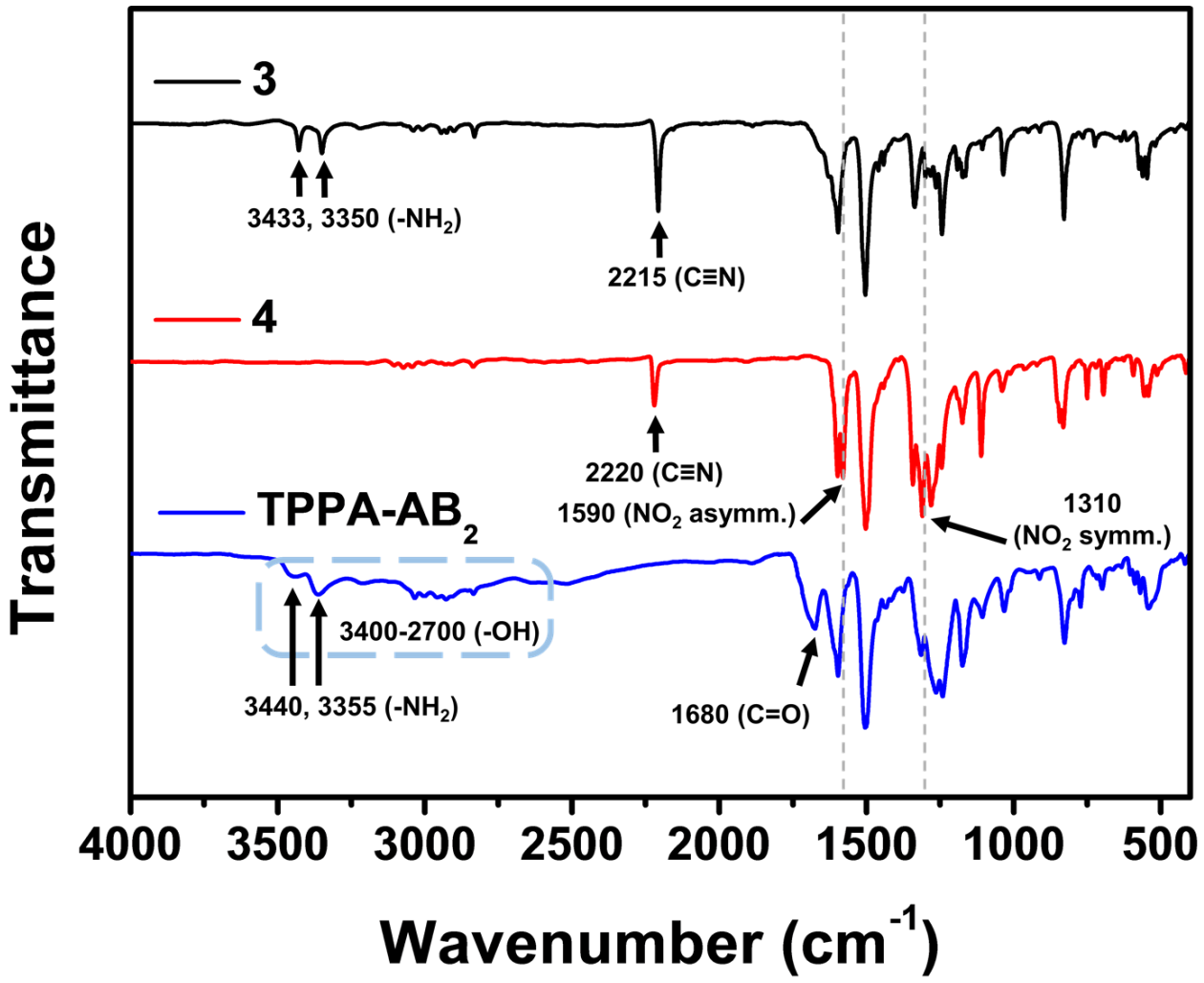

Fig. S1. FT-IR spectra of compounds **3**, **4**, and **TPPA-AB2**.

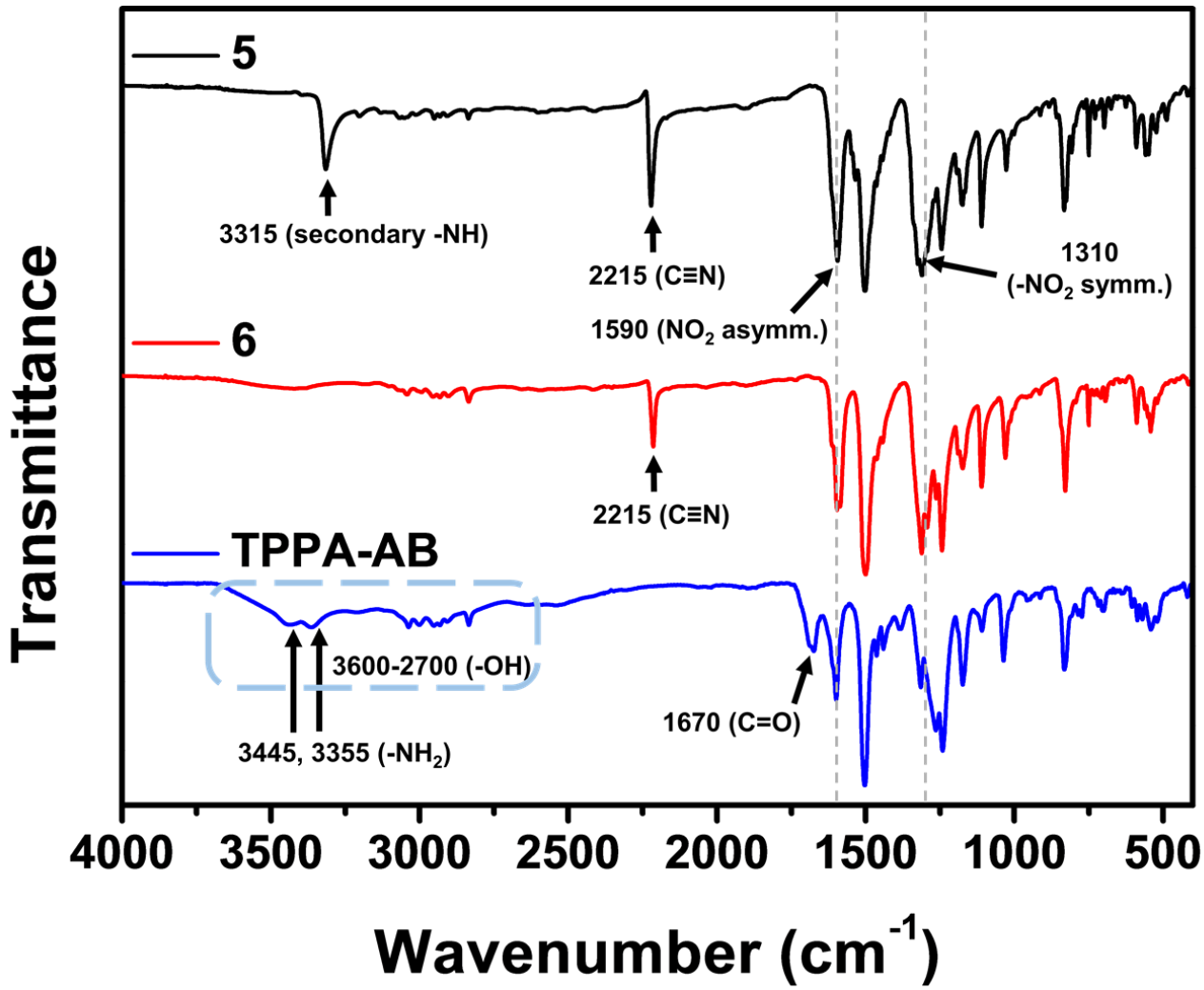

Fig. S2. FT-IR spectra of compounds **5**, **6**, and **TPPA-AB**.

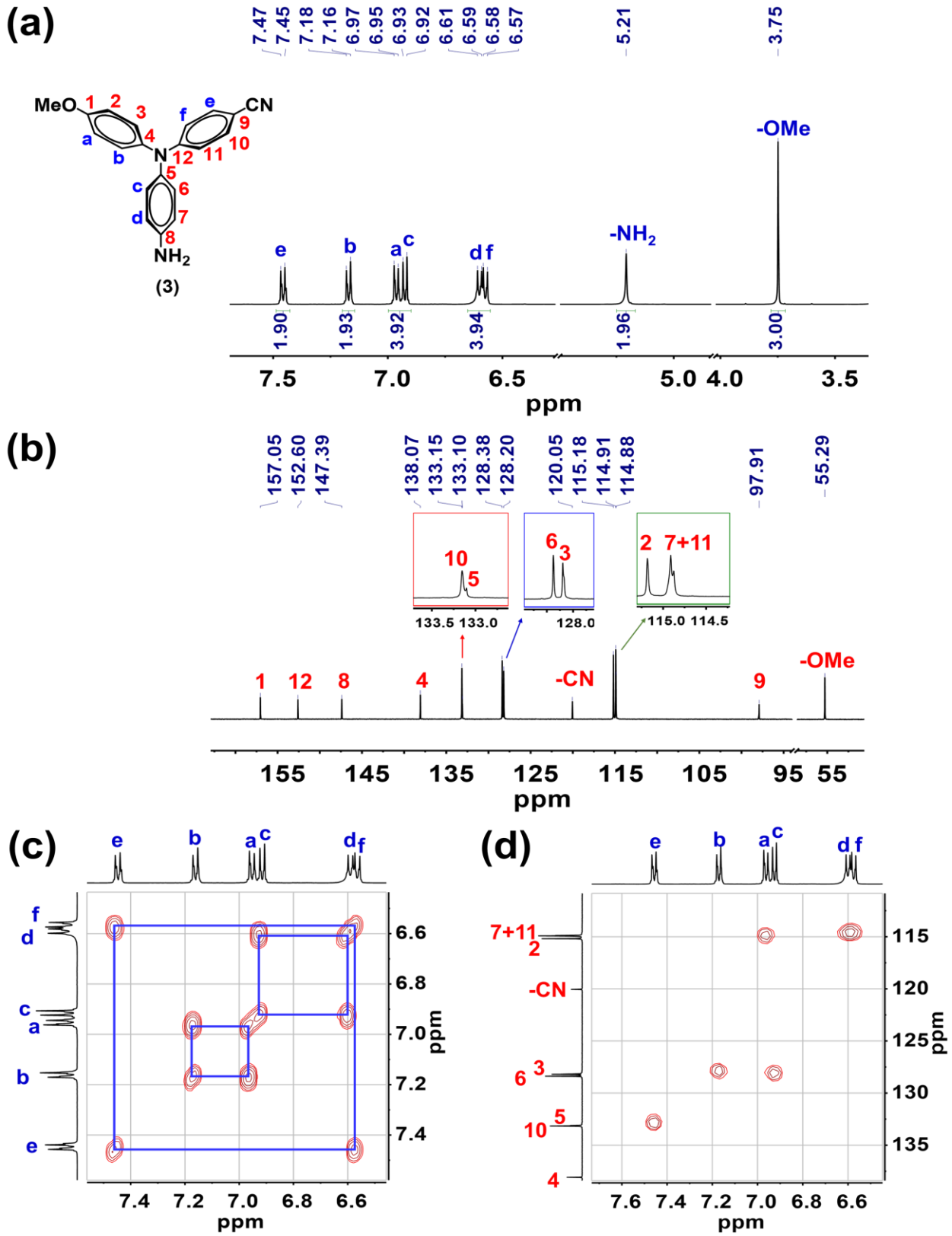

Fig. S3. (a) ^{1}H-NMR, (b) ^{13}C-NMR, (c) ^{1}H-^{1}H COSY NMR, and (d) ^{13}C-^{1}H HSQC NMR spectra of compound **3** in DMSO-d_6.

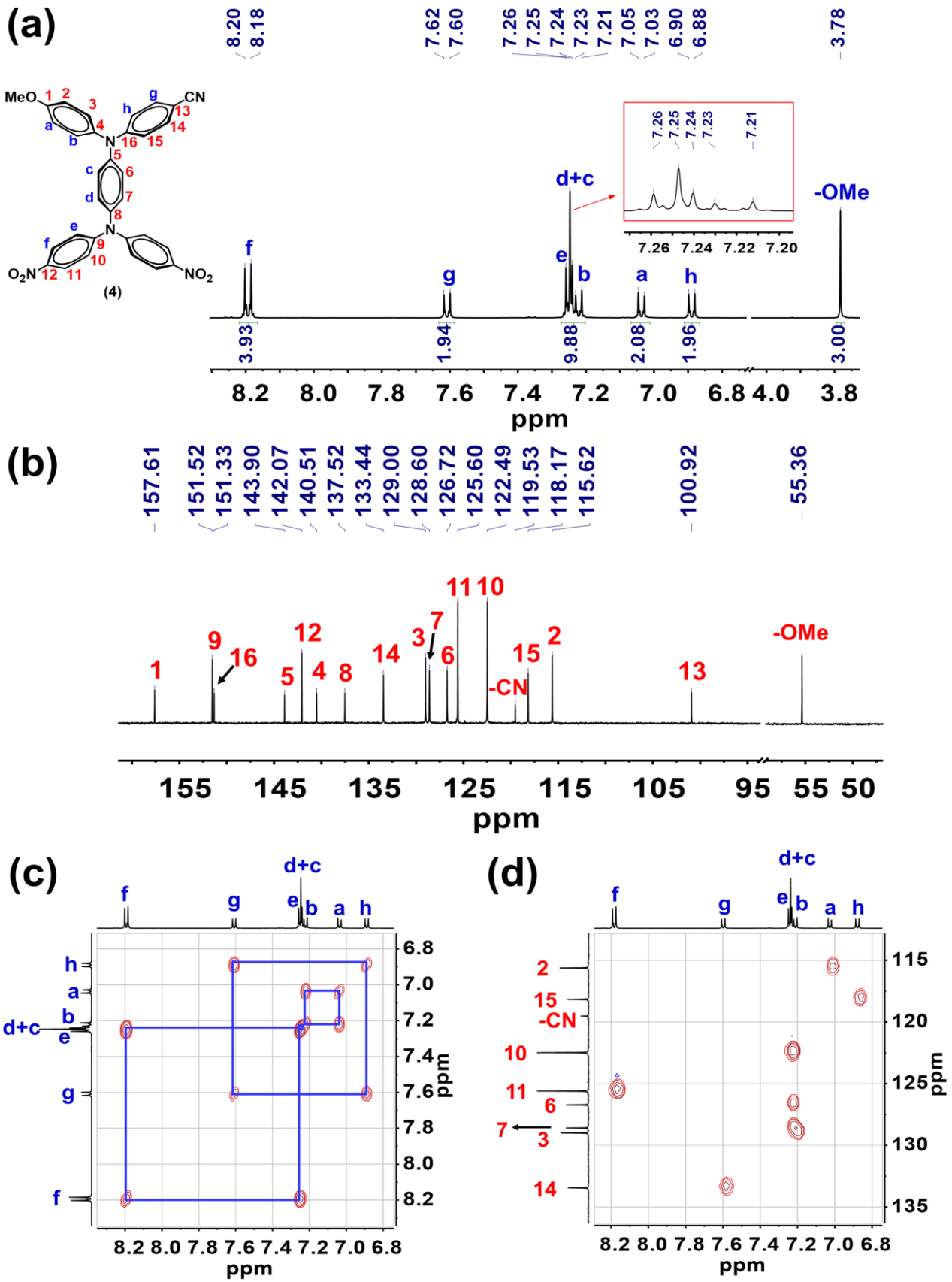

Fig. S4. (a) ^{1}H-NMR, (b) ^{13}C-NMR, (c) ^{1}H-^{1}H COSY NMR, and (d) ^{13}C-^{1}H HSQC NMR spectra of compound **4** in DMSO-d_6.

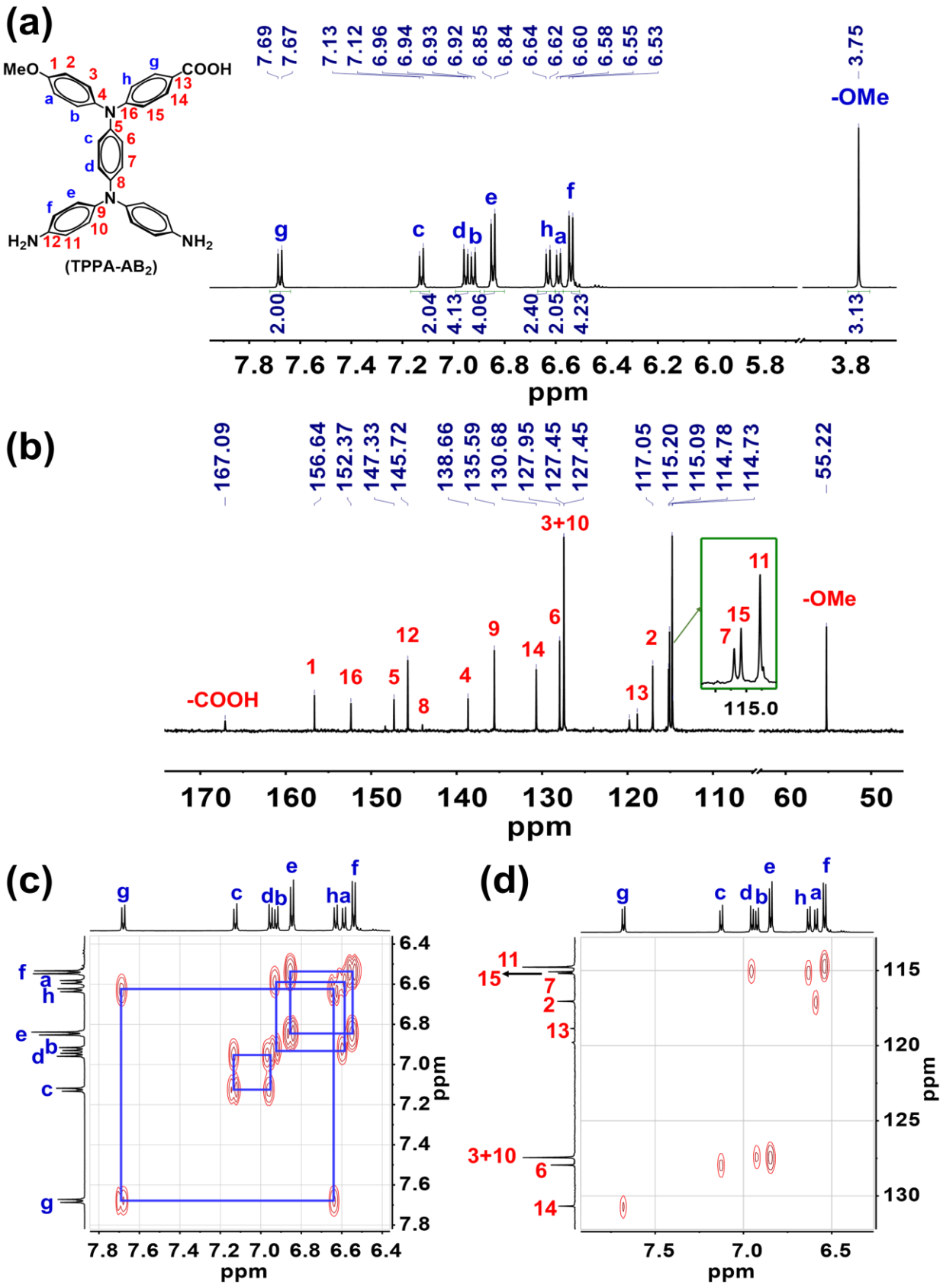

Fig. S5. (a) ^{1}H-NMR, (b) ^{13}C-NMR, (c) ^{1}H-^{1}H COSY NMR, and (d) ^{13}C-^{1}H HSQC NMR spectra of compound **TPPA-AB$_2$** in DMSO-d_6.

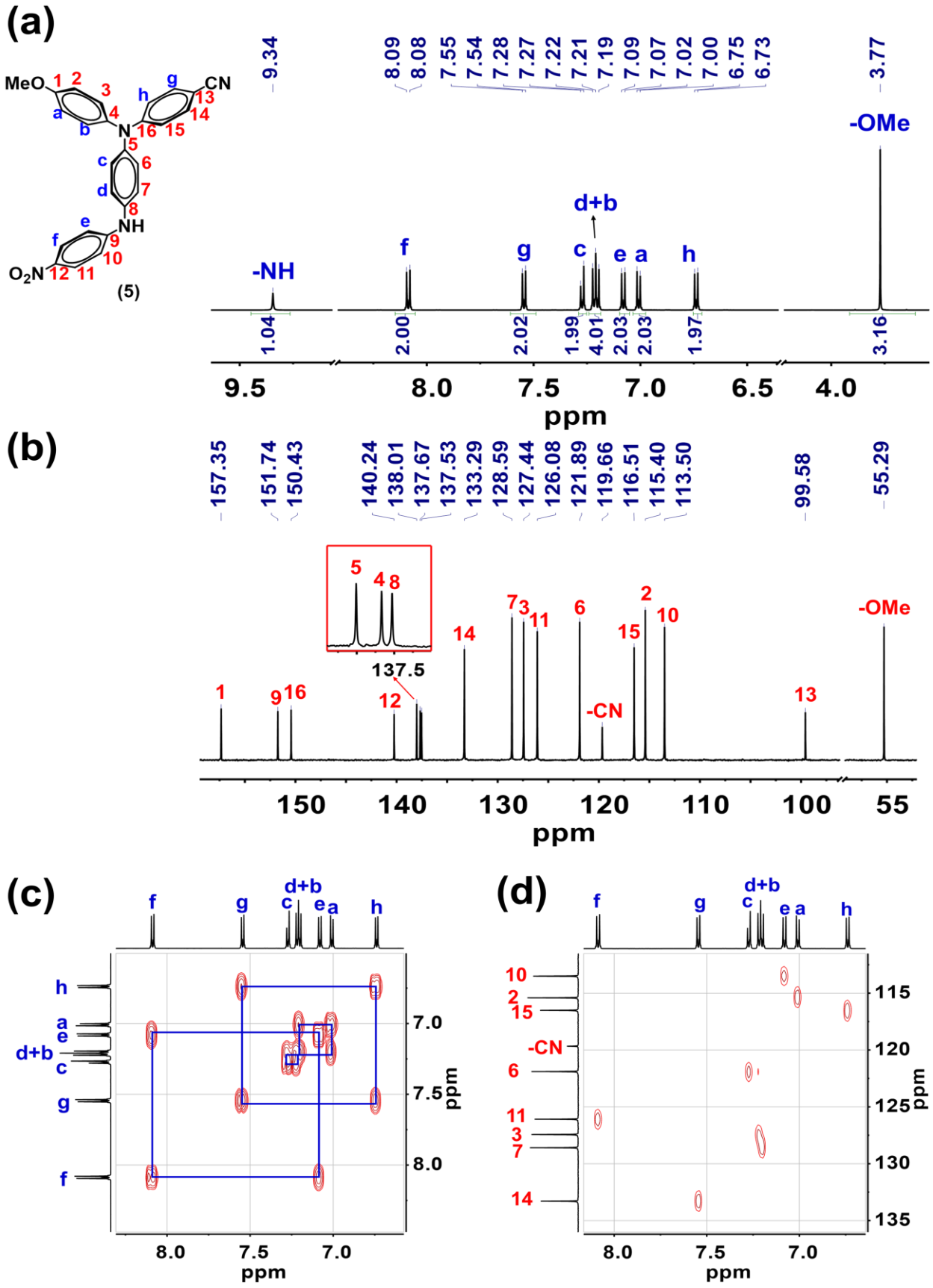

Fig. S6. (a) ^{1}H-NMR, (b) ^{13}C-NMR, (c) ^{1}H-^{1}H COSY NMR, and (d) ^{13}C-^{1}H HSQC NMR spectra of compound **5** in DMSO-d_6.

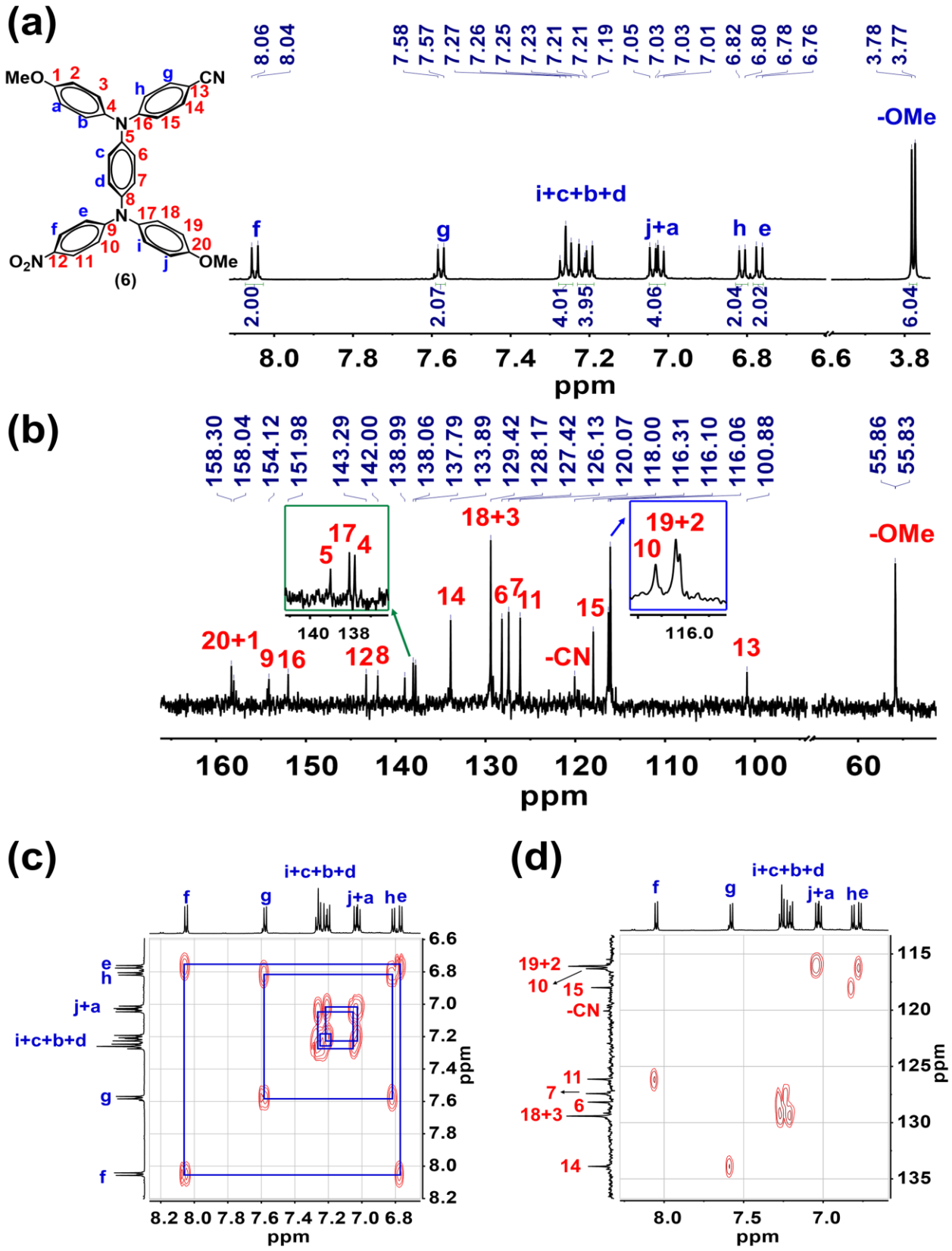

Fig. S7. (a) ^{1}H-NMR, (b) ^{13}C-NMR, (c) ^{1}H-^{1}H COSY NMR, and (d) ^{13}C-^{1}H HSQC NMR spectra of compound **6** in DMSO-d_6.

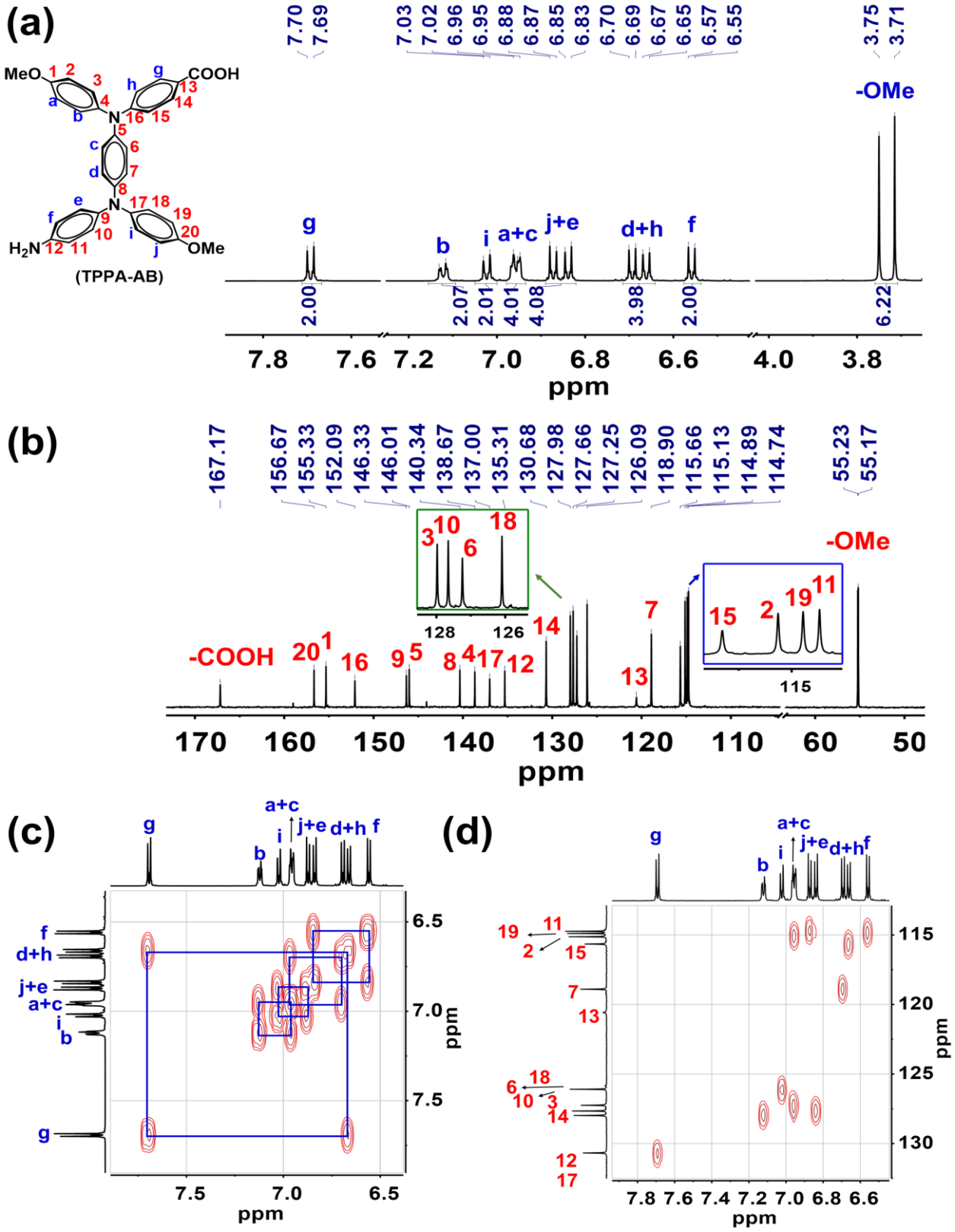

Fig. S8. (a) ^{1}H-NMR, (b) ^{13}C-NMR, (c) ^{1}H-^{1}H COSY NMR, and (d) ^{13}C-^{1}H HSQC NMR spectra of compound **TPPA-AB** in DMSO-d_6.

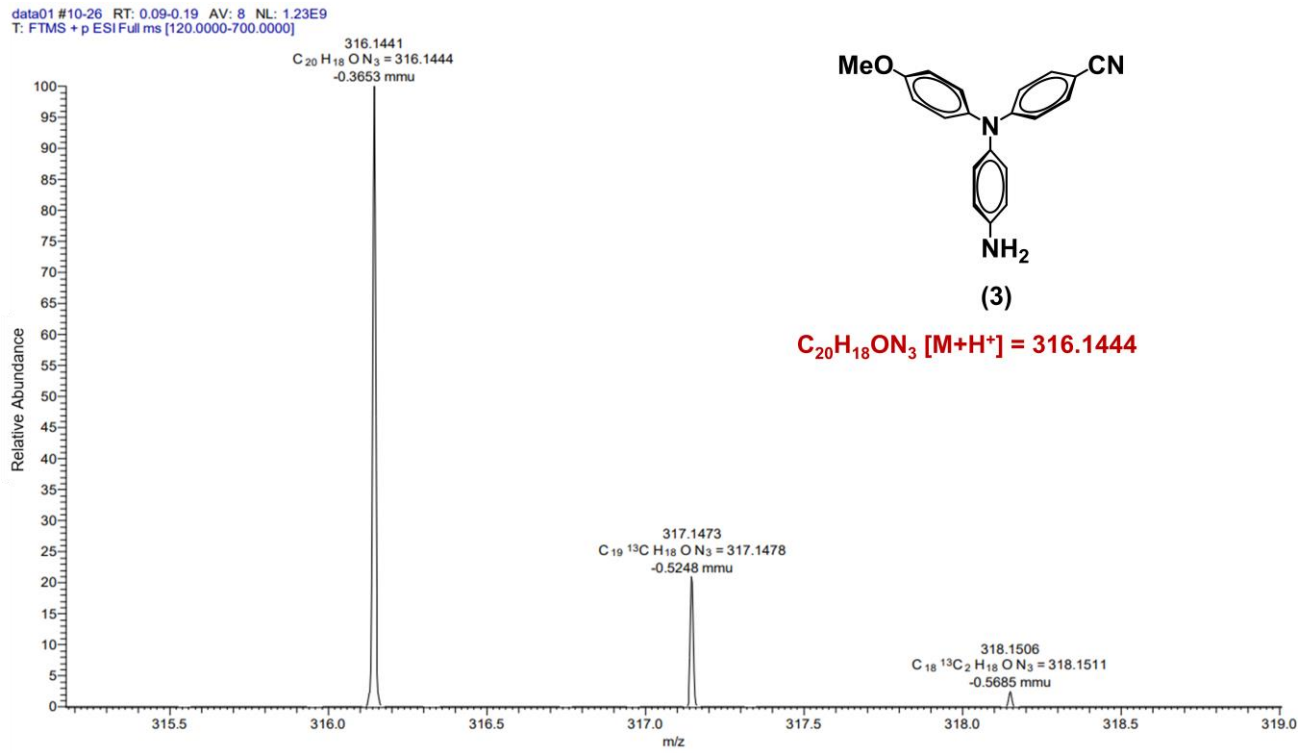

Fig. S9. HRMS report of compound **3**.

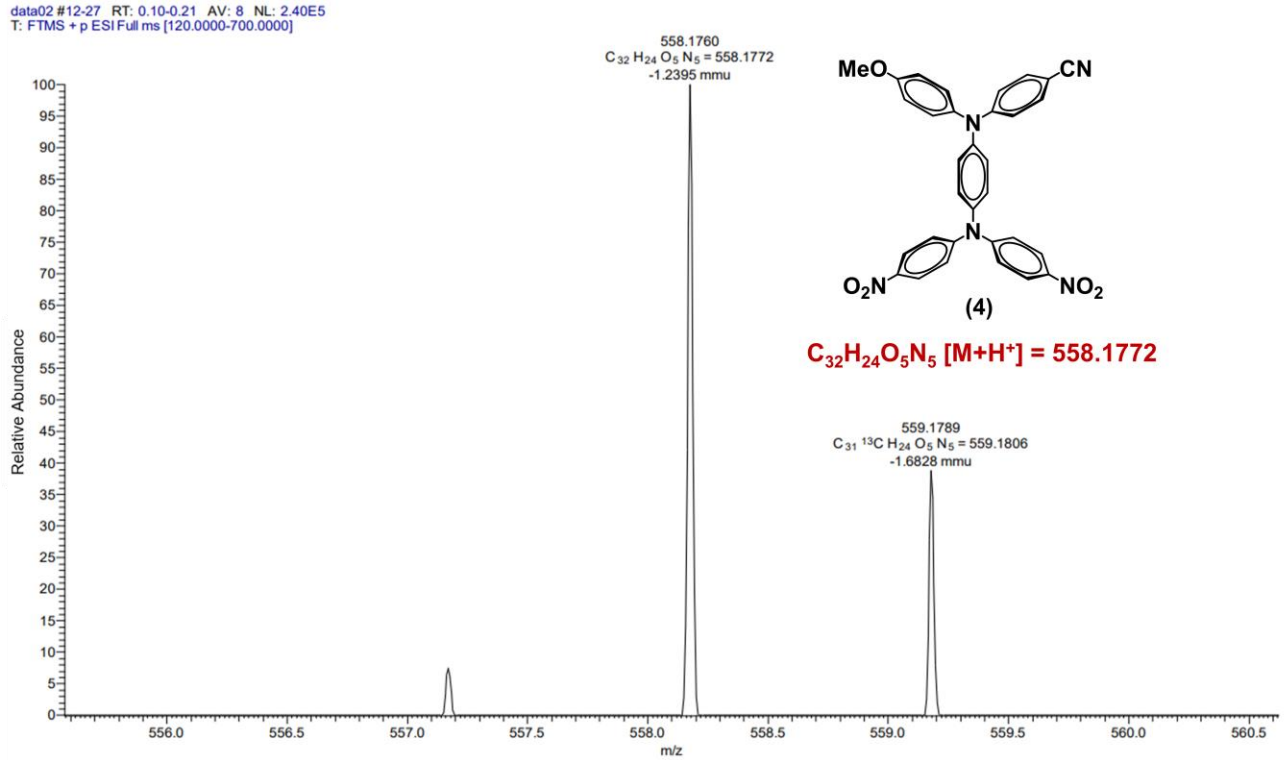

Fig. S10. HRMS report of compound **4**.

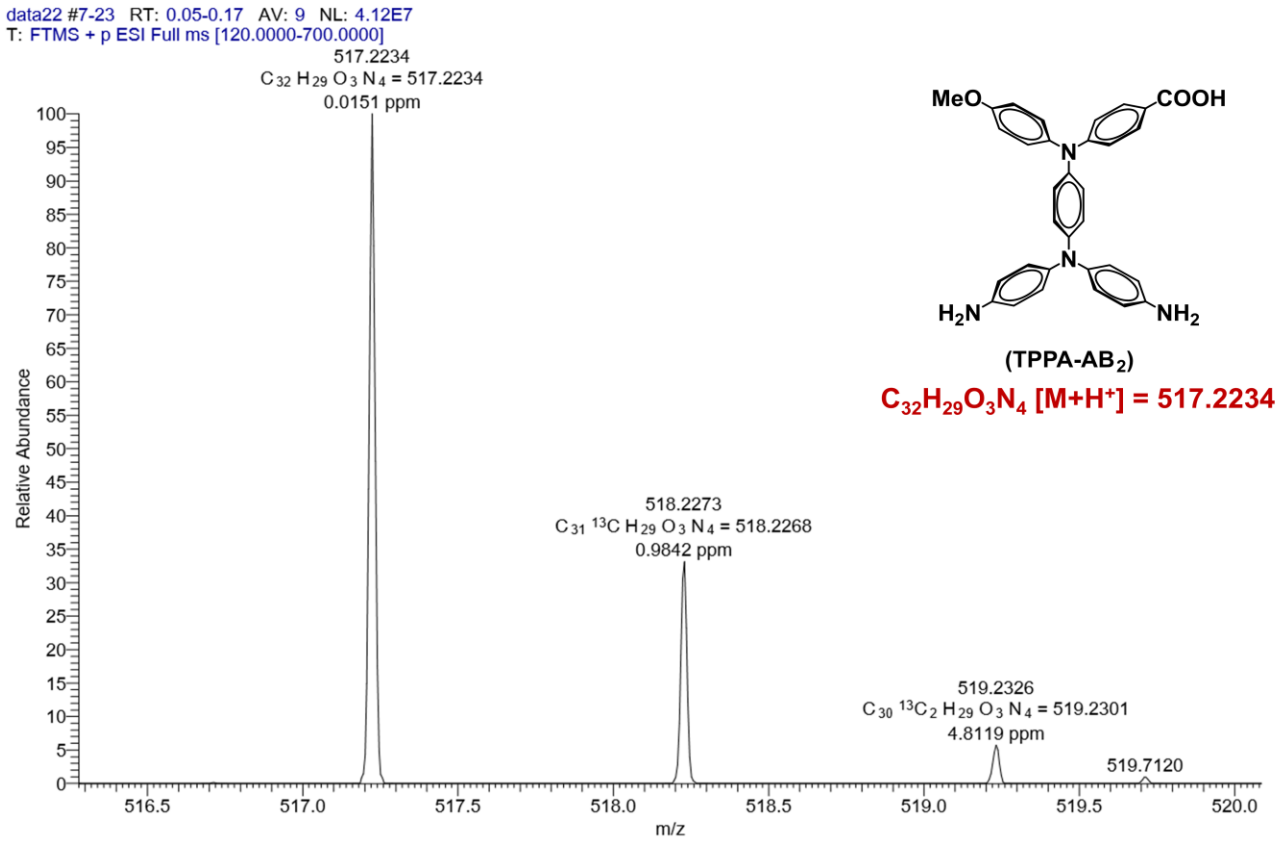

Fig. S11. HRMS report of **TPPA-AB$_2$**.

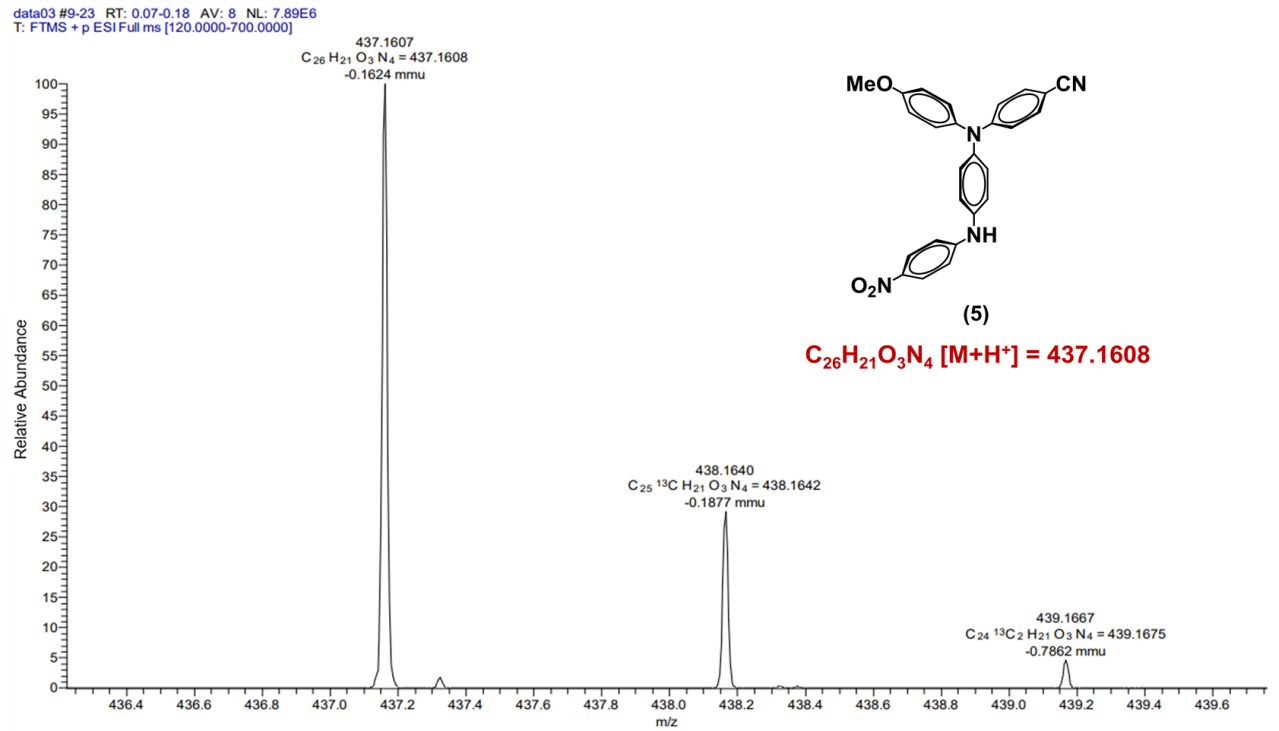

Fig. S12. HRMS report of compound **5**.

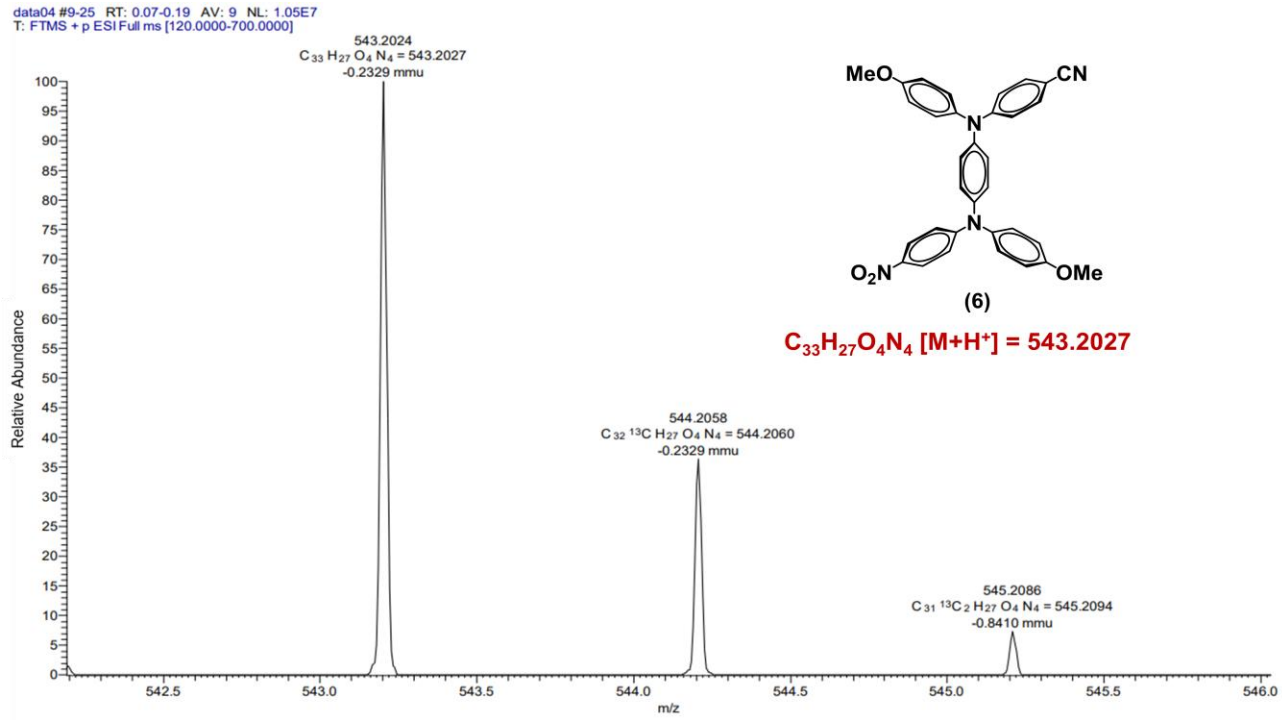

Fig. S13. HRMS report of compound **6**.

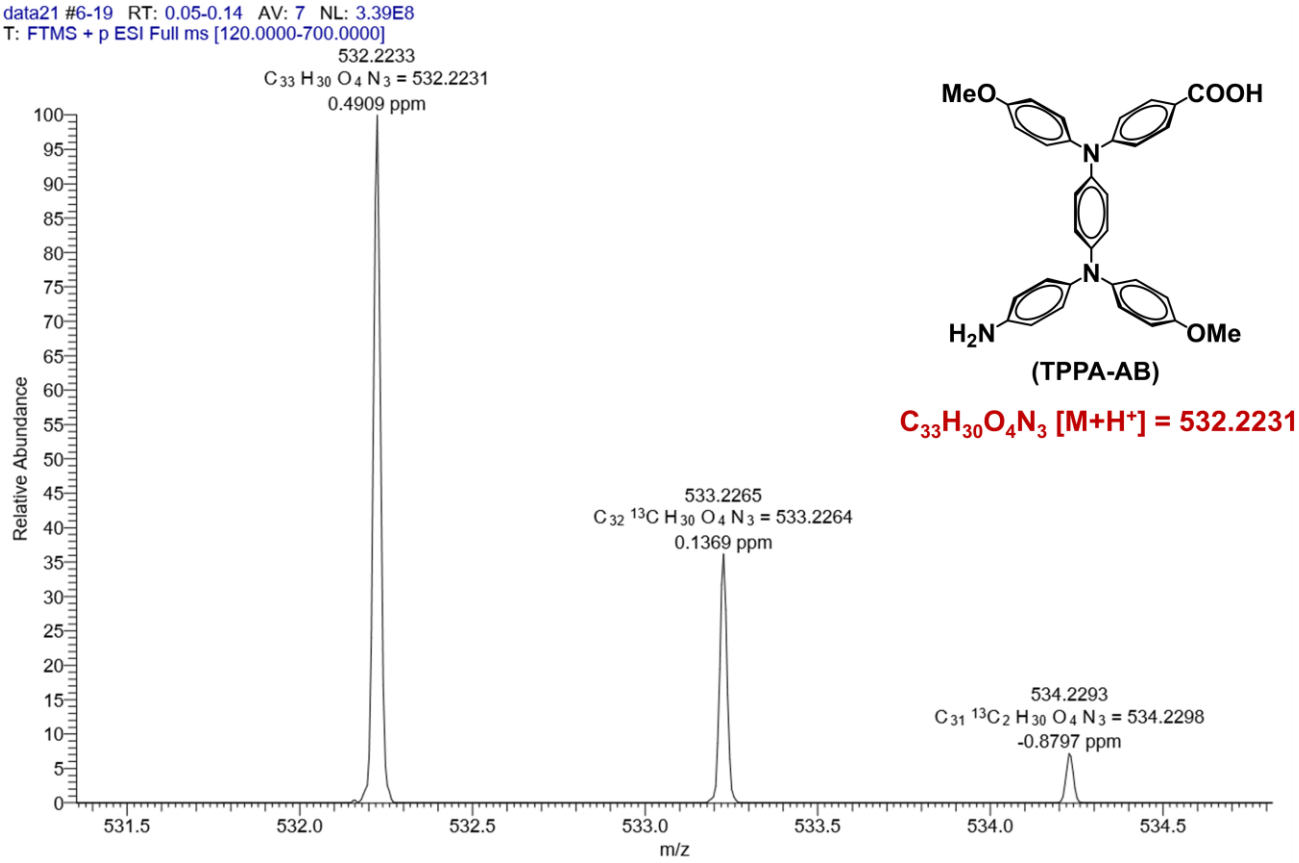

Fig. S14. HRMS report of **TPPA-AB**.

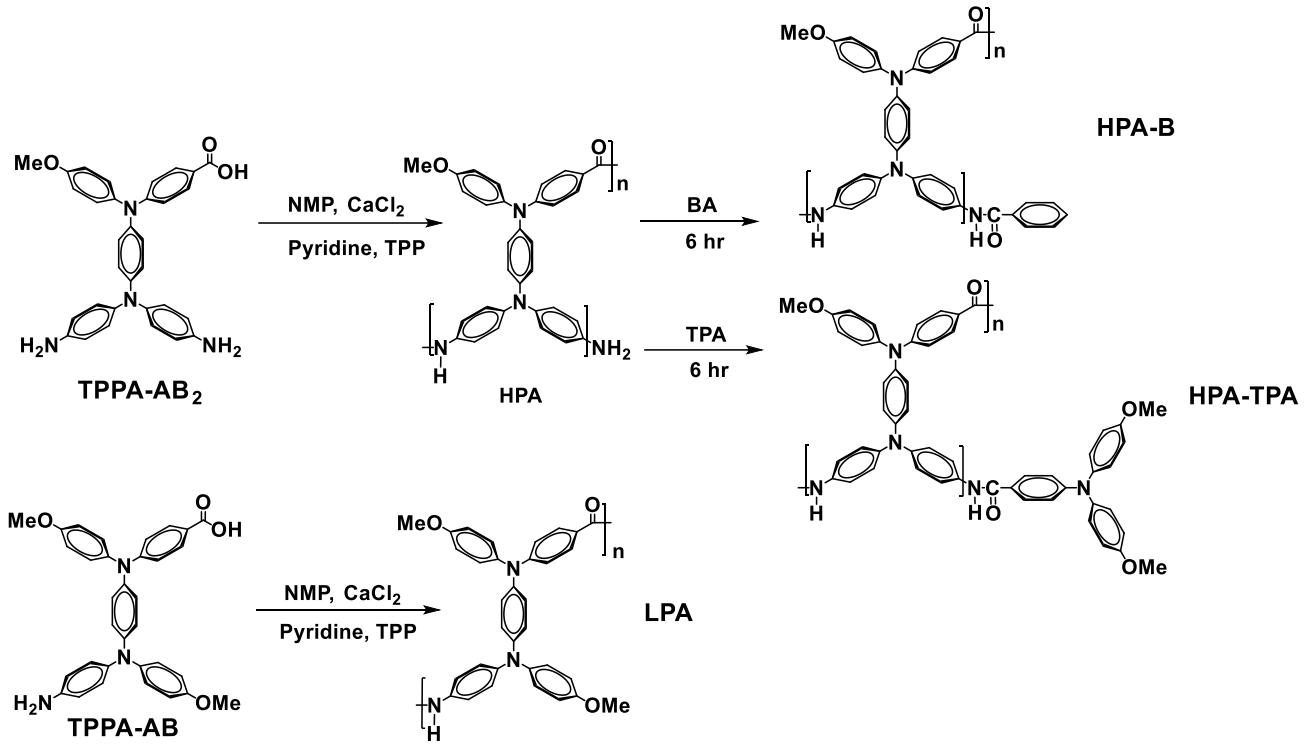

Scheme S2. The synthetic route and picture of hyperbranched polyamides **HPA-TPA**, **HPA-B** and linear polyamide **LPA**.

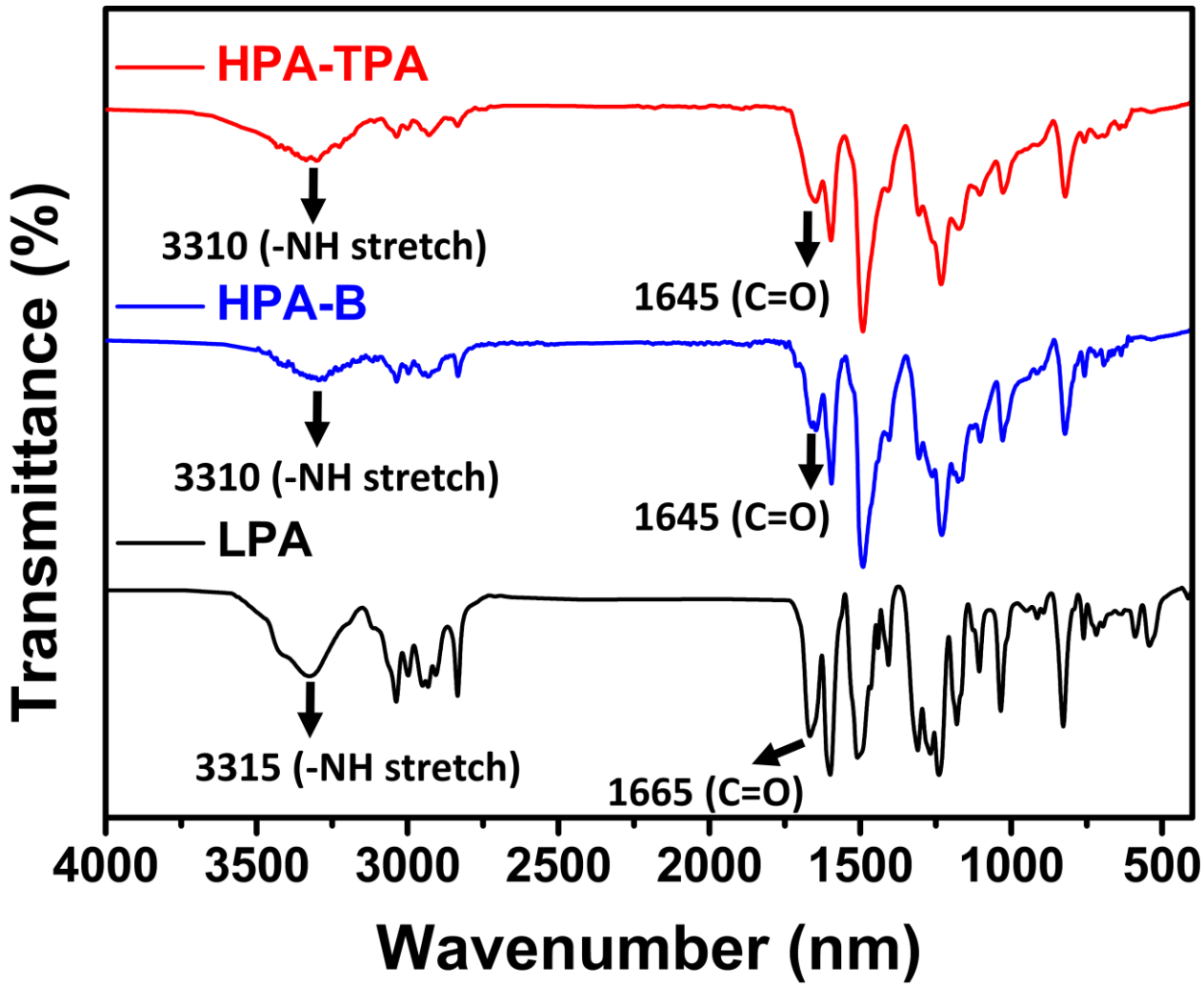

Fig. S15. FT-IR spectra of polyamide films **HPA-TPA**, **HPA-B** and **LPA**.

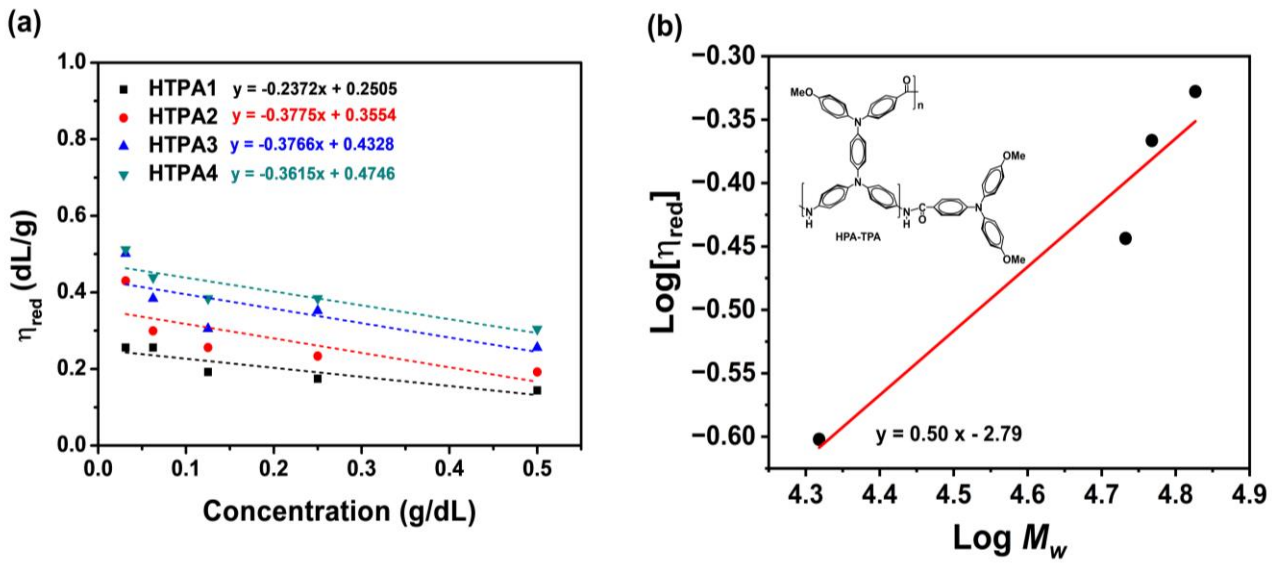

Fig. S16. (a) The reduced viscosity of **HTPA1-4** vs. concentrations is used to calculate intrinsic viscosity. (b) Relationships between log [η] vs. log Mw of **HTPA1-4**. The α value was obtained from the slope of the fitting line.

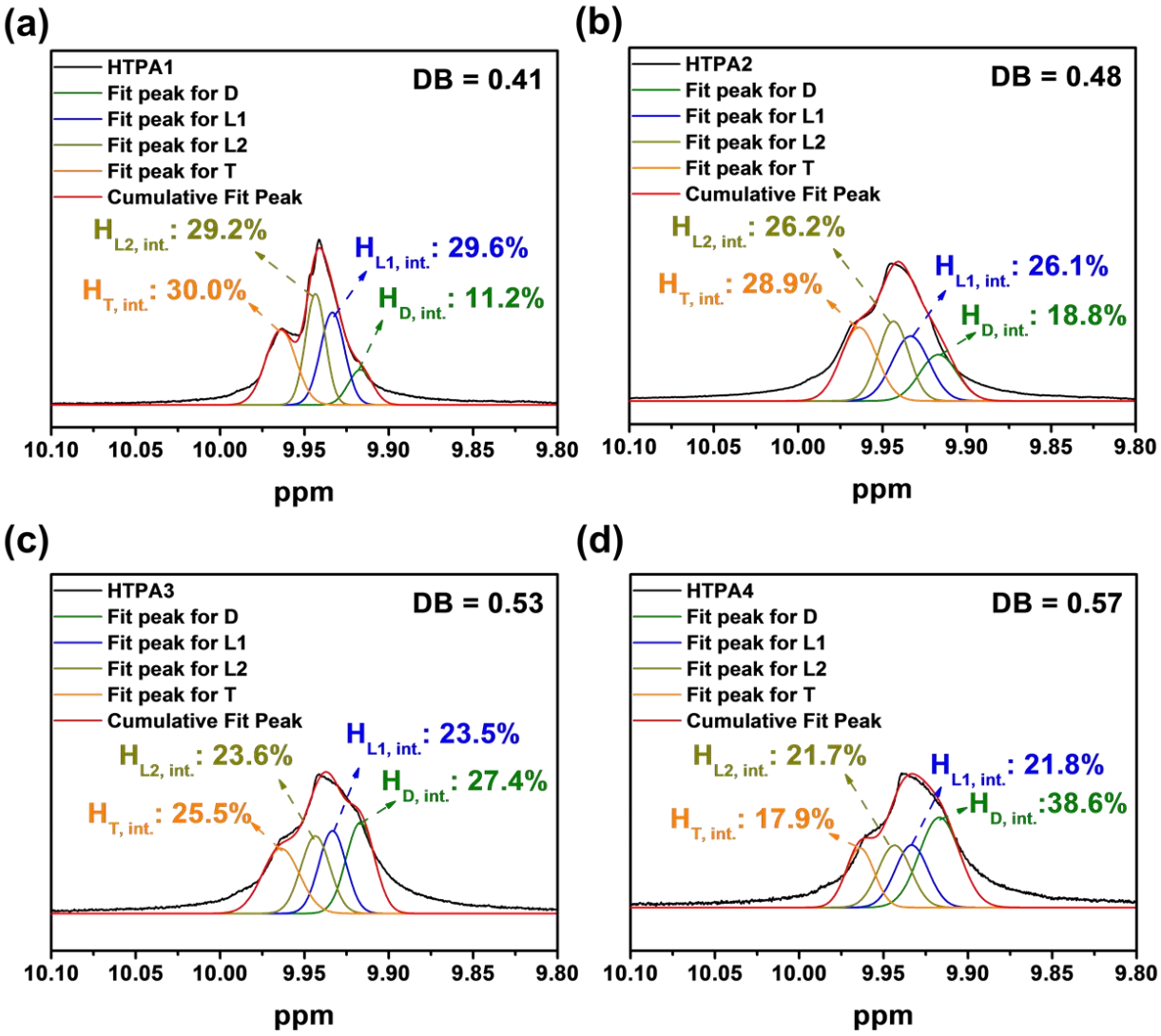

Fig. S17. Deconvolution of the ^{1}H-NMR spectra (solid black lines) for **HTPA1-4** in one pot with different reaction times 30, 60, 80, and 100 min following 6 hours end-capping reaction with contributions area (green: dendritic, blue, dark yellow: linear, and orange: terminal) as well as the resulting total simulation (red) are shown as well.

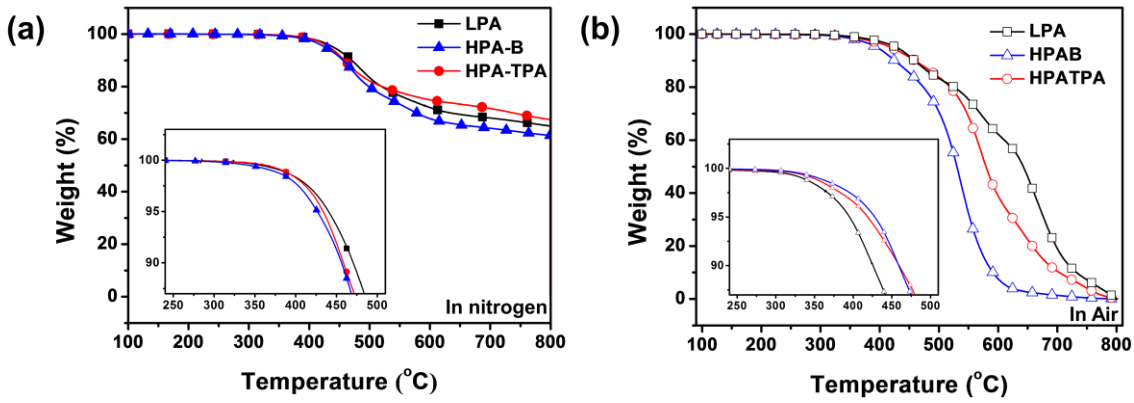

Fig. S18. TGA curves of prepared polymers under (a) nitrogen and (b) air atmosphere.

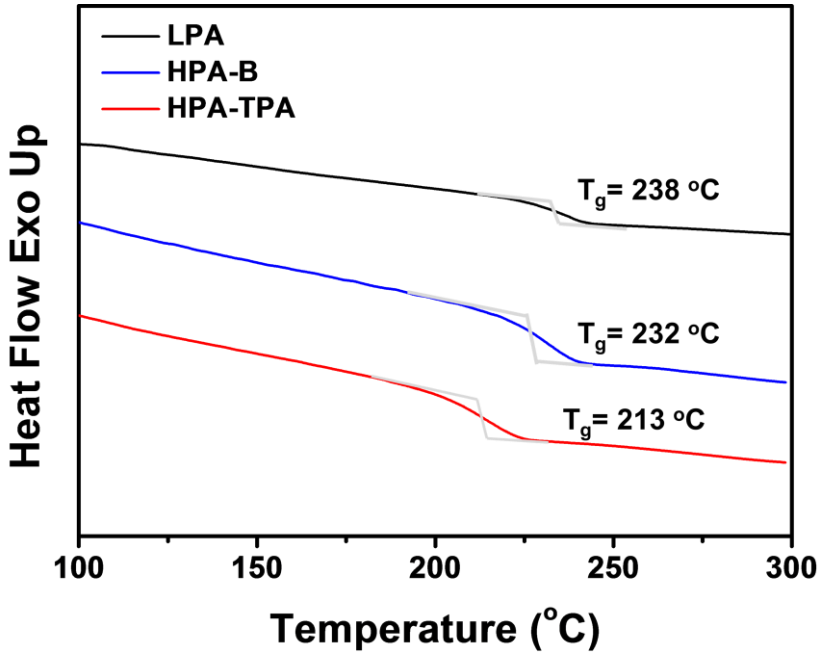

Fig. S19. DSC 2nd trace of polyamides at the heating rate of 20 °C/min in a nitrogen atmosphere.

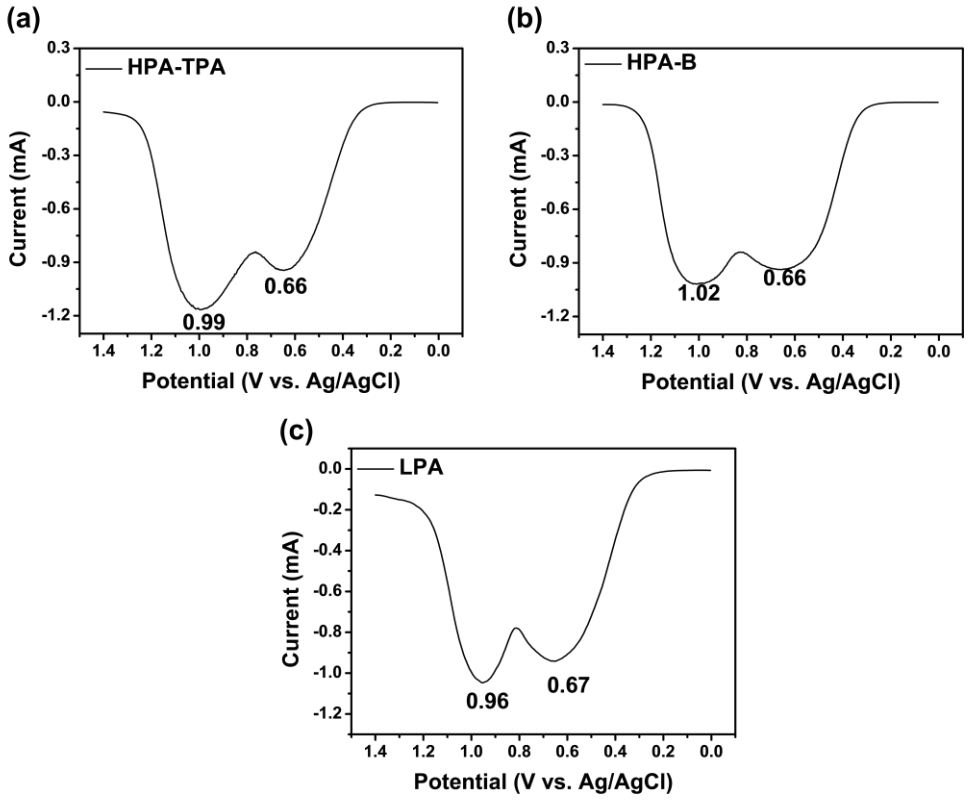

Fig. S20. DPV diagrams of (a) **HPA-TPA** (thickness: 310 ± 30 nm), (b) **HPA-B** (thickness: 300 ± 20 nm), and (c) **LPA** (thickness: 300 ± 20 nm), measured on the ITO-coated glass substrate (coated area: 0.6 cm × 3 cm) with 0.1 M $TBABF_4$ in MeCN. Scan rate: 4 mV s^{-1}; pulse amplitude: 50 mV; pulse width: 50 ms; pulse period: 0.5 s.

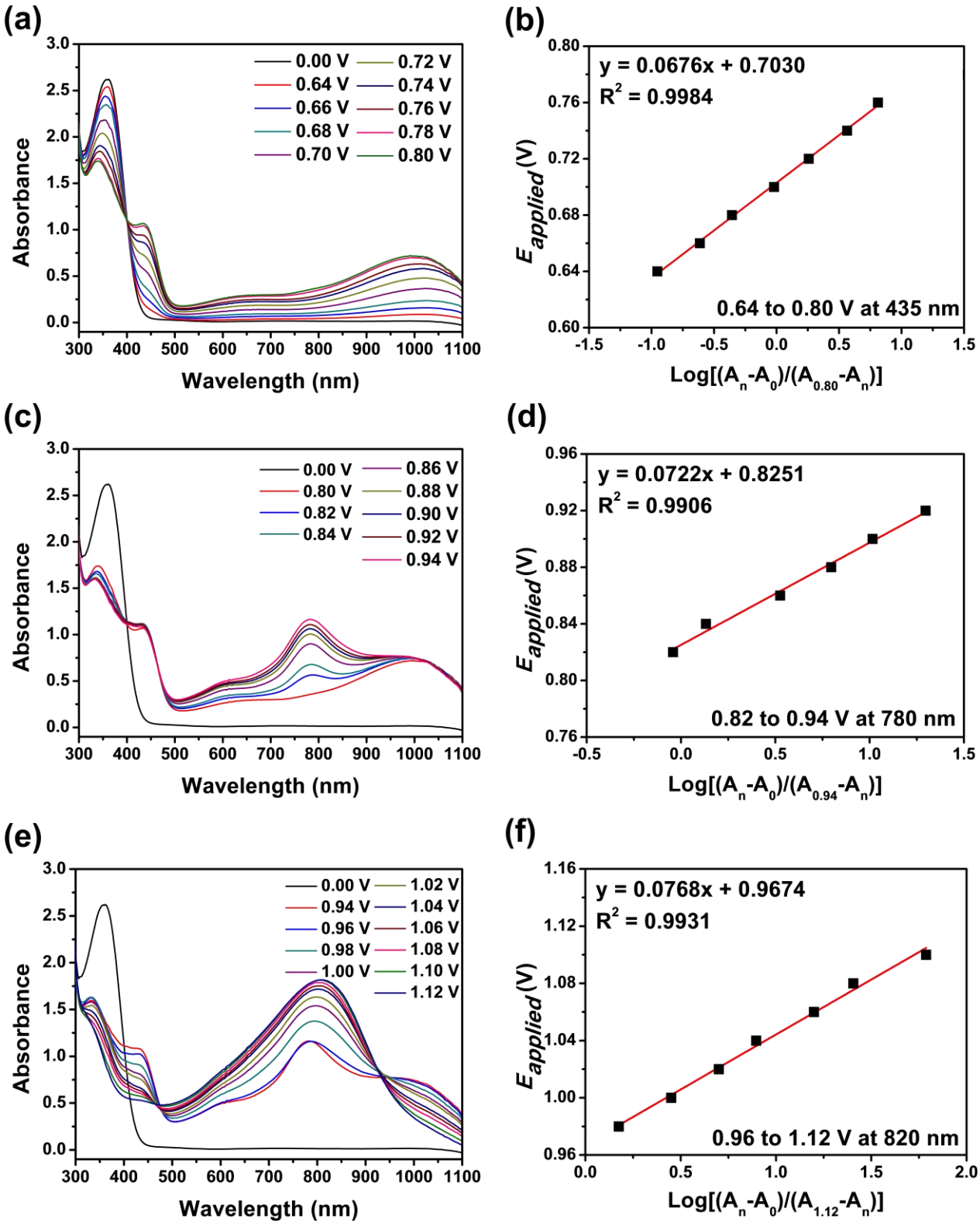

Fig. S21. Absorption spectral change for **HPA-TPA** film and $E_{applied}$ vs. $\log[(A_n - A_0)/(A_{max} - A_n)]$ plot at the applied potential from (a and b) 0.64-0.80 V, (c and d) 0.82-0.94 V, (e and f) 0.94-1.12V measured on an ITO-coated glass substrate with 0.1 M $TBABF_4$ in 3 mL MeCN (V vs. Ag/AgCl).

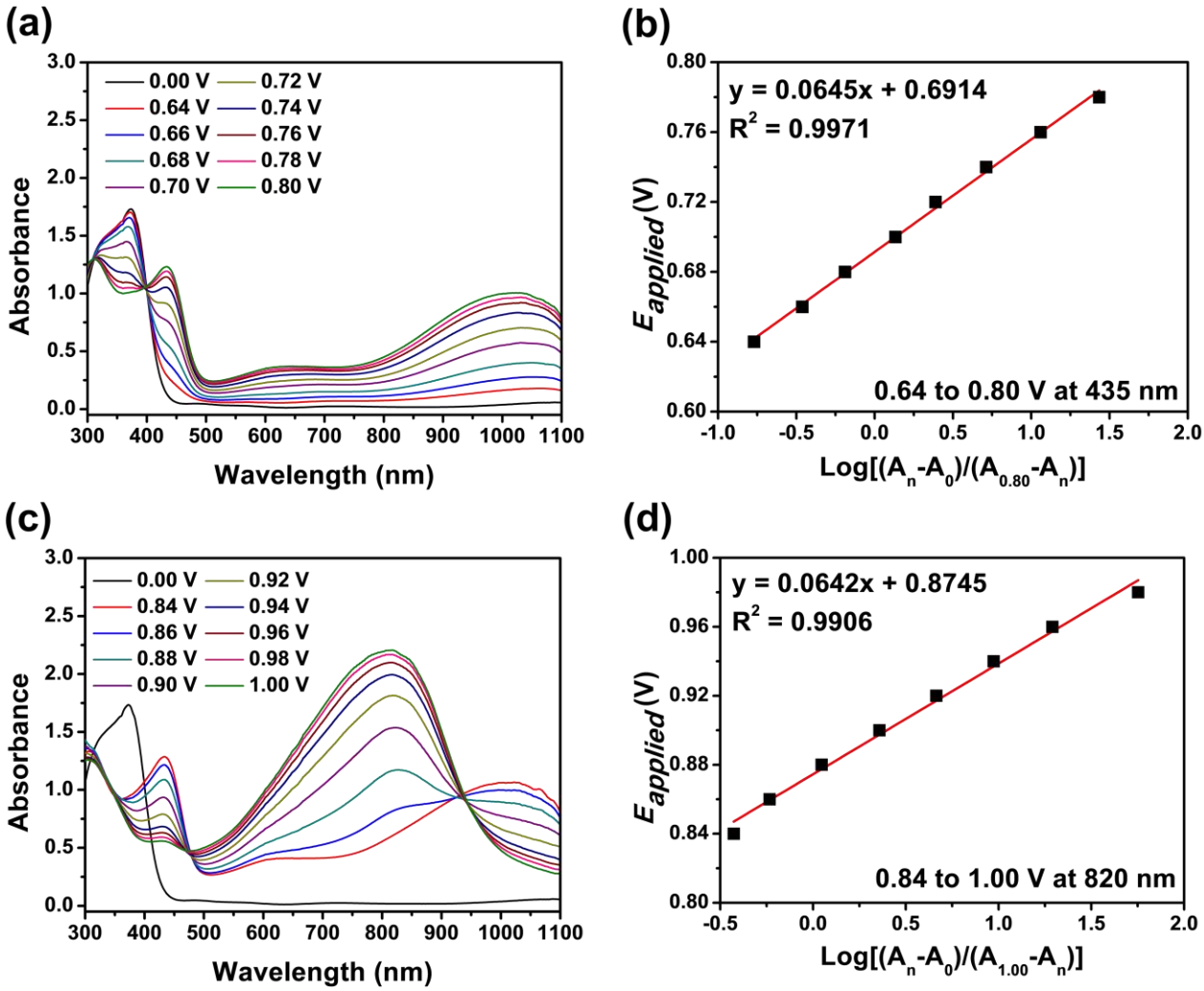

Fig. S22. Absorption spectral change for **HPA-B** film and $E_{applied}$ vs. $\log[(A_n - A_0)/(A_{max} - A_n)]$ plot at the applied potential from (a and b) 0.64-0.80 V, (c and d) 0.84-1.00 V measured on an ITO-coated glass substrate with 0.1 M $TBABF_4$ in 3 mL MeCN (V vs. Ag/AgCl).

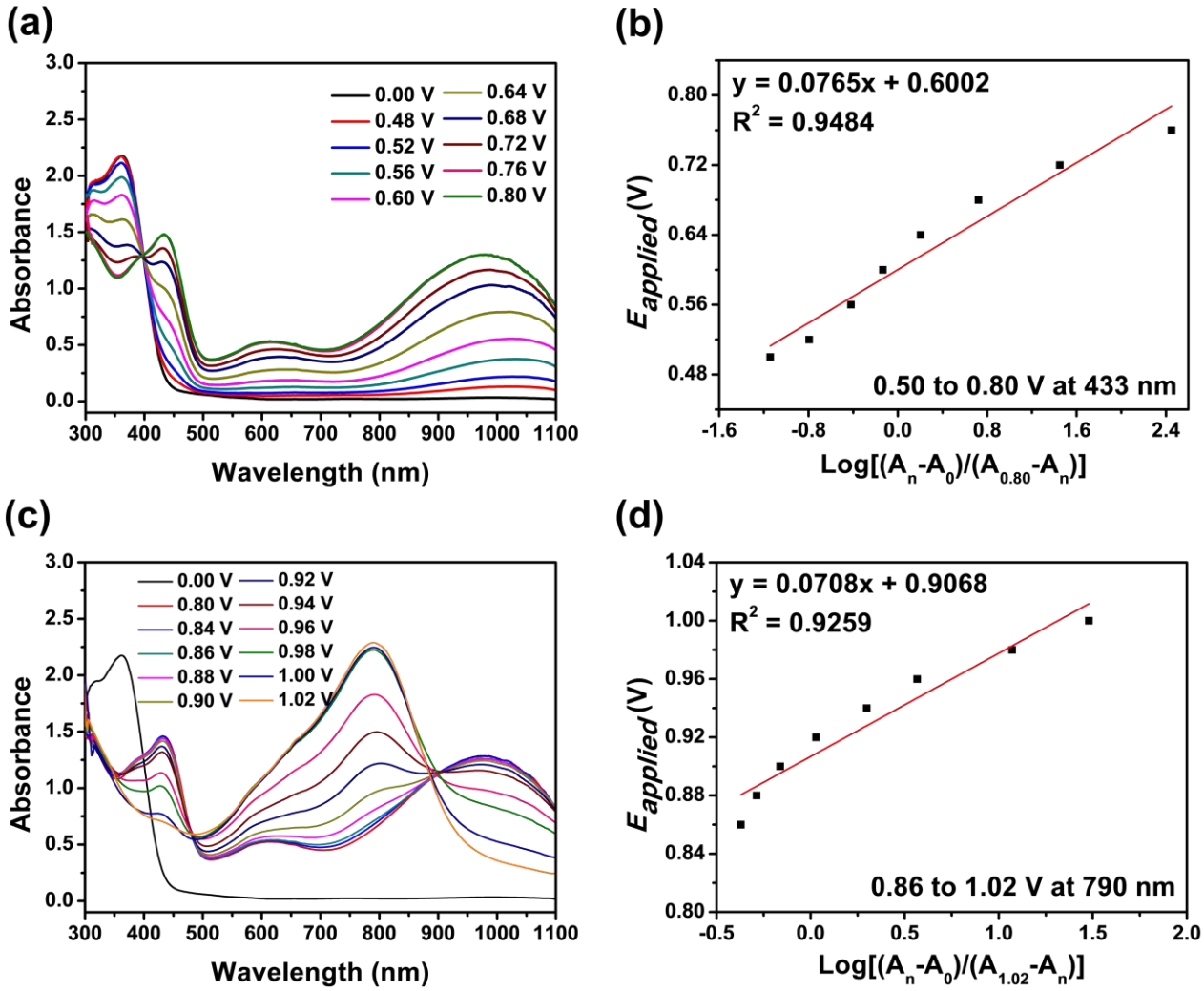

Fig. S23. Absorption spectral change for **LPA** film and $E_{applied}$ vs. log[$(A_n - A_0)/(A_{max} - A_n)$] plot at the applied potential from (a and b) 0.50-0.80 V, (c and d) 0.86-1.02 V measured on an ITO-coated glass substrate with 0.1 M $TBABF_4$ in 3 mL MeCN (V vs. Ag/AgCl).

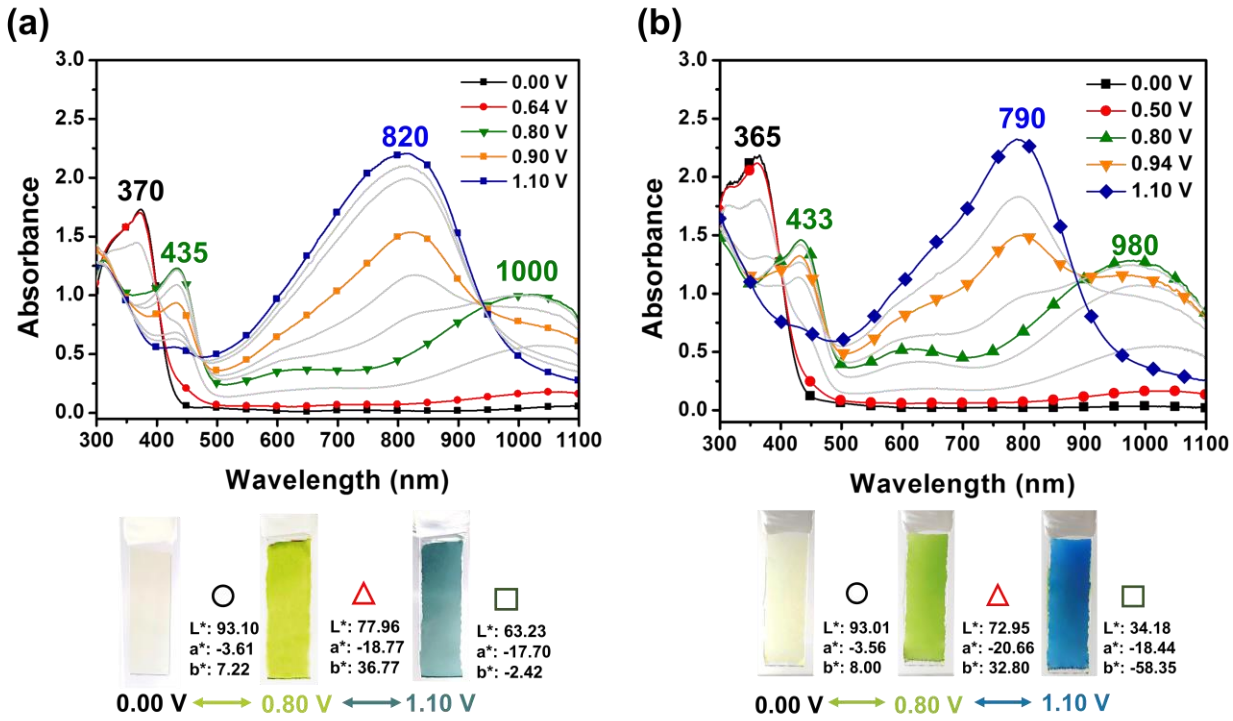

Fig. S24. Spectroelectrochemical spectra and the analysis of CIELAB colour space for (a) **HPA-B** and (b) **LPA** measured on the ITO-coated glass substrate in 0.1 M $TBABF_4$/MeCN.

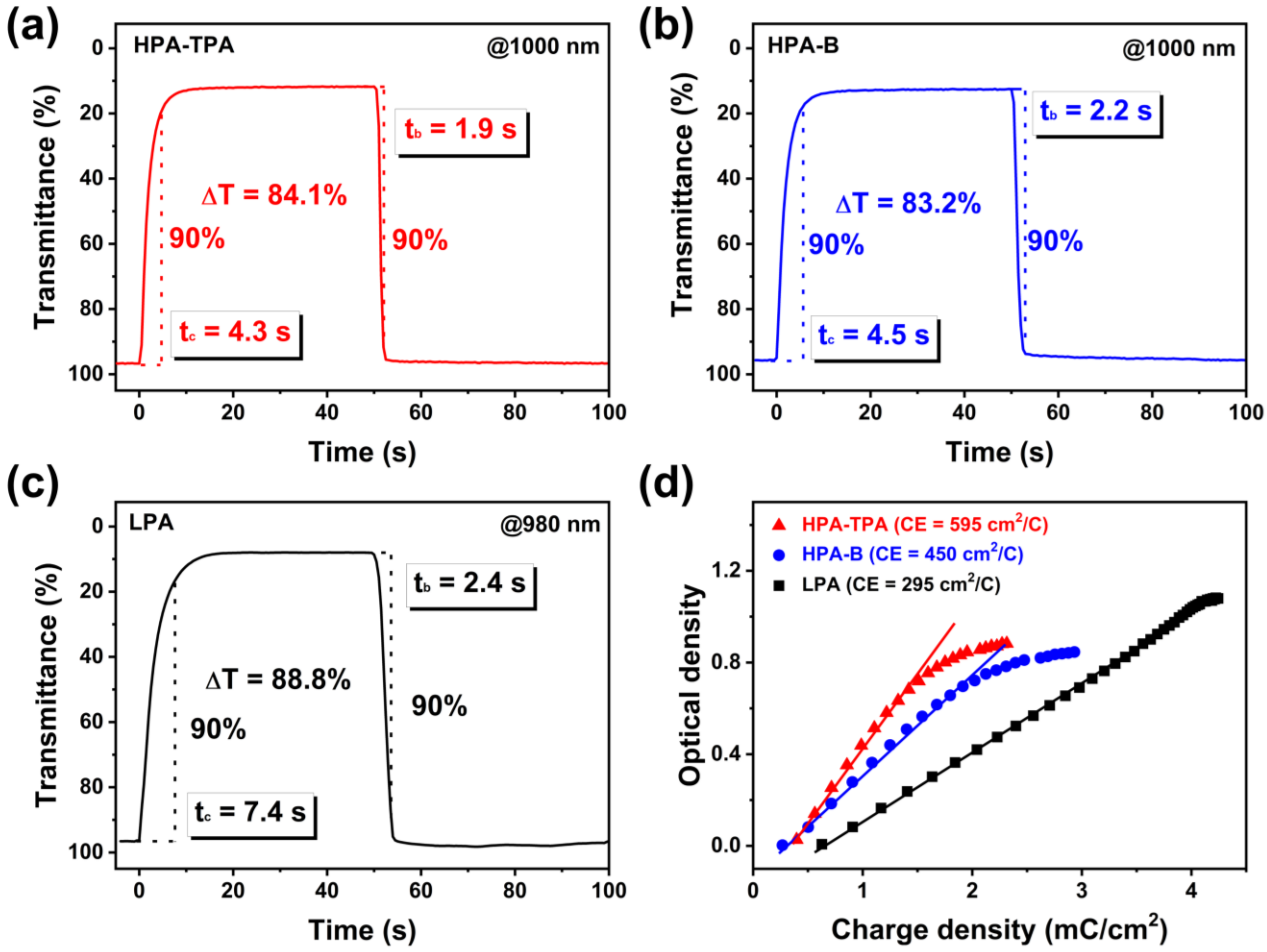

Fig. S25. Switching response time between −0.3 to 0.8 V (a) **HPA-TPA** (@ 1000 nm), (b) **HPA-B** (@ 1000 nm), and (c) **LPA** (@ 980 nm) with a cycle time of 100 s on the ITO-coated glass substrate in 0.1 M $TBABF_4$/MeCN. (d) Optical density *vs.* charge density polymer films in the coloration process to obtain coloration efficiency by the fitting slope.

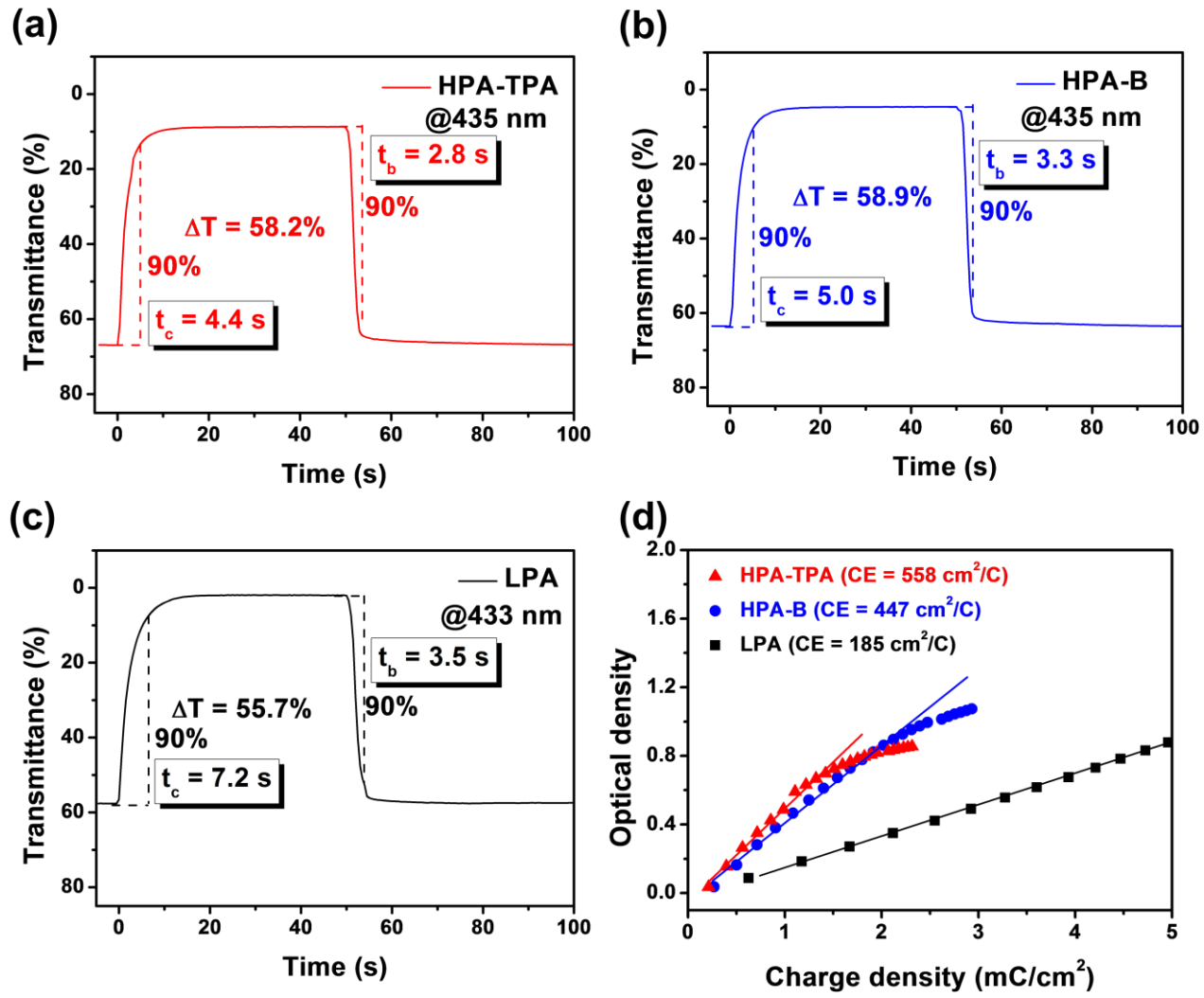

Fig. S26. Switching response time between −0.3 to 0.8 V (a) **HPA-TPA** (@ 435 nm), (b) **HPA-B** (@ 435 nm), and (c) **LPA** (@ 433 nm) with a cycle time of 100 s on the ITO-coated glass substrate in 0.1 M $TBABF_4$/MeCN. (d) Optical density *vs.* charge density polymer films in the coloration process to obtain coloration efficiency by the fitting slope.

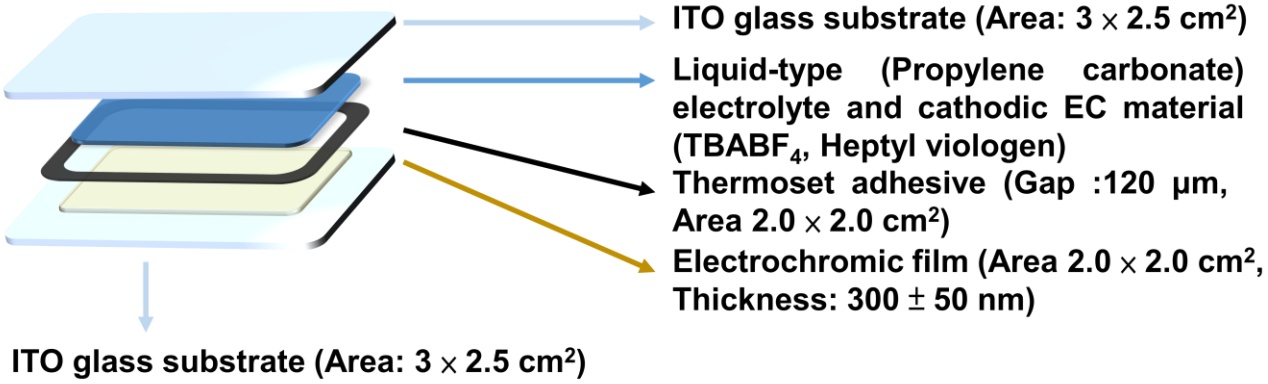

Fig. S27. Schematic diagram of the fabricated electrochromic devices.

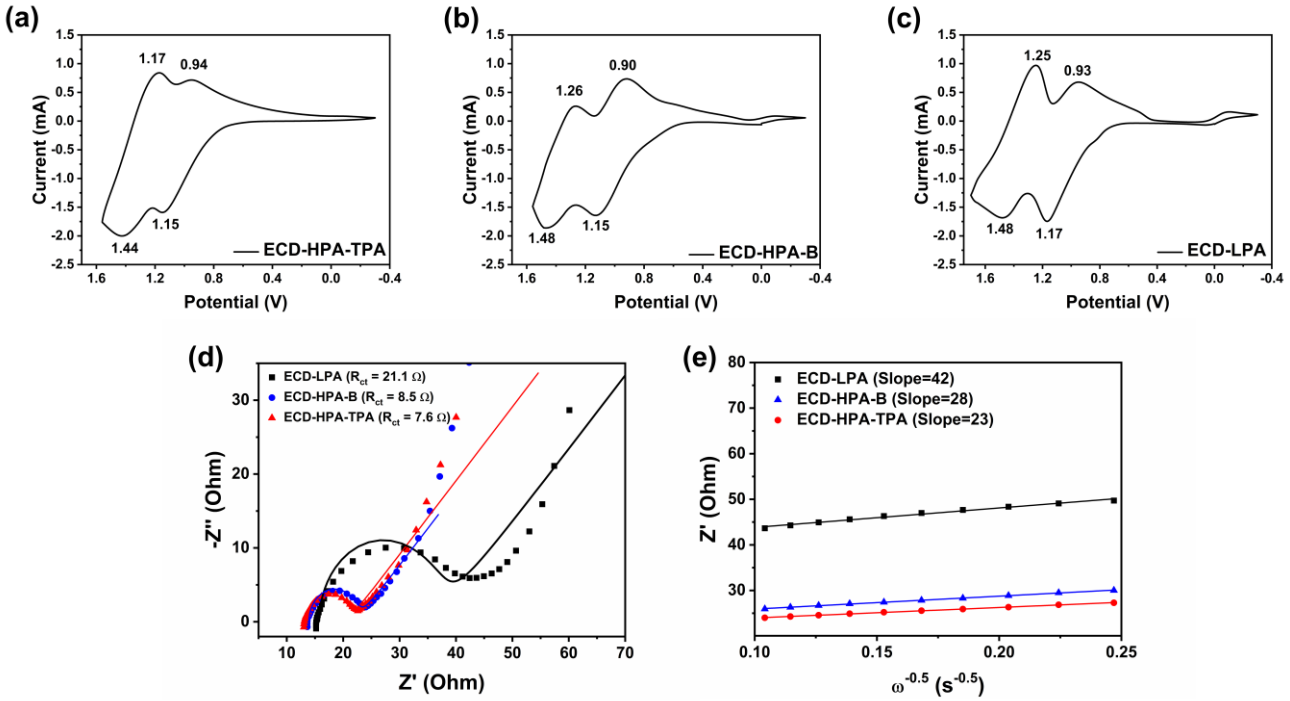

Fig. S28. CV diagrams of the ECDs derived from (a) **ECD-HPA-TPA** (thickness: 330 ± 30 nm), (b) **ECD-HPA-B** (thickness: 320 ± 20 nm), and (c) **ECD-LPA**. (d) Nyquist plots fitting with Randles equivalent circuit (solid lines are the fitted lines) and (e) the fitted linear plot between Z′ and $\omega^{-0.5}$ at the low-frequency region under the oxidation state of the prepared devices. (thickness: 350 ± 20 nm) on the ITO-coated glass substrate (coated area: 2 cm x 2 cm) in about 48 µL propylene carbonate with 0.1 M $TBABF_4$ as electrolyte and 0.015 M $HV(BF_4)_2$.

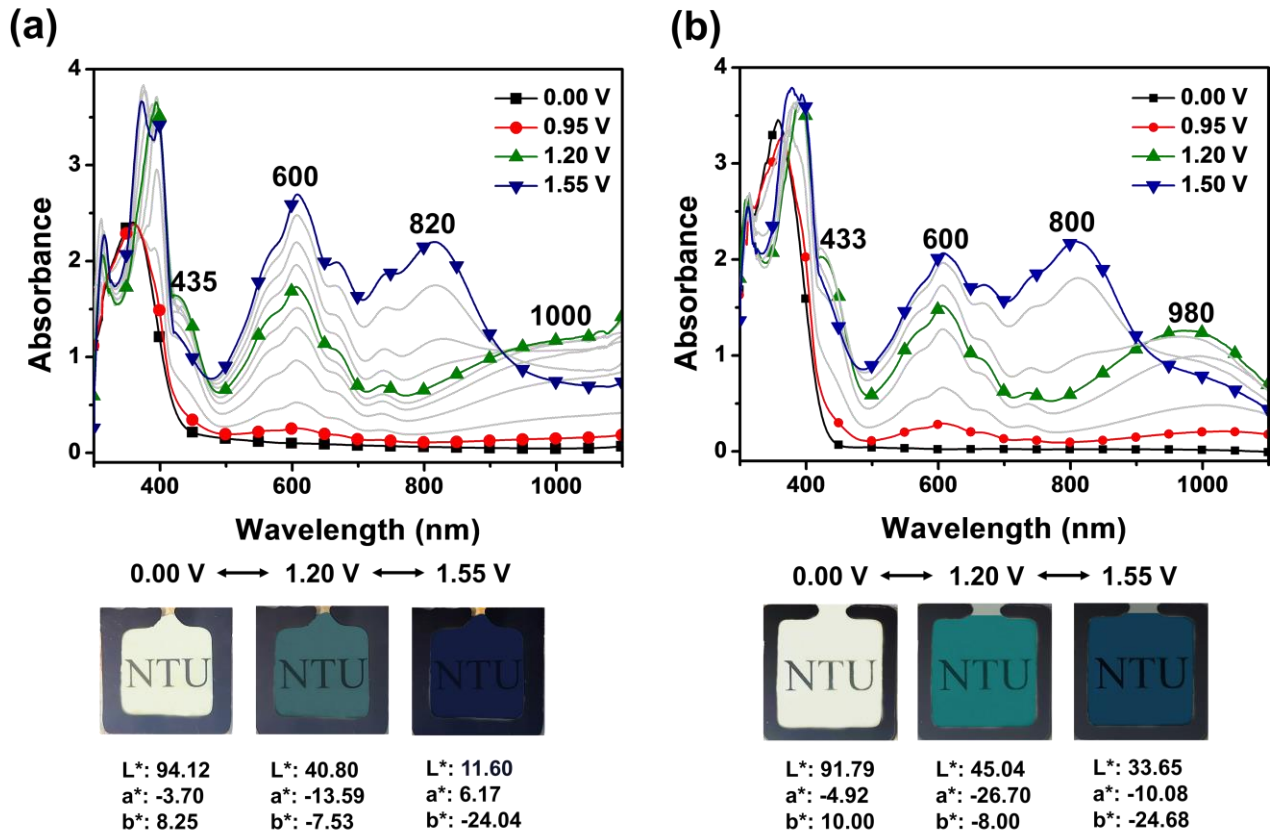

Fig. S29. Spectroelectrochemistry behaviour of the ECDs (a) **ECD-HPA-B** (thickness: 320 ± 20 nm) and (b) **ECD-LPA** (thickness: 350 ± 20 nm) on the ITO-coated glass (coated area: 2 cm × 2 cm) substrate in about 48 μL propylene carbonate with 0.1 M $TBABF_4$ as electrolyte and 0.015 M $HV(BF_4)_2$.

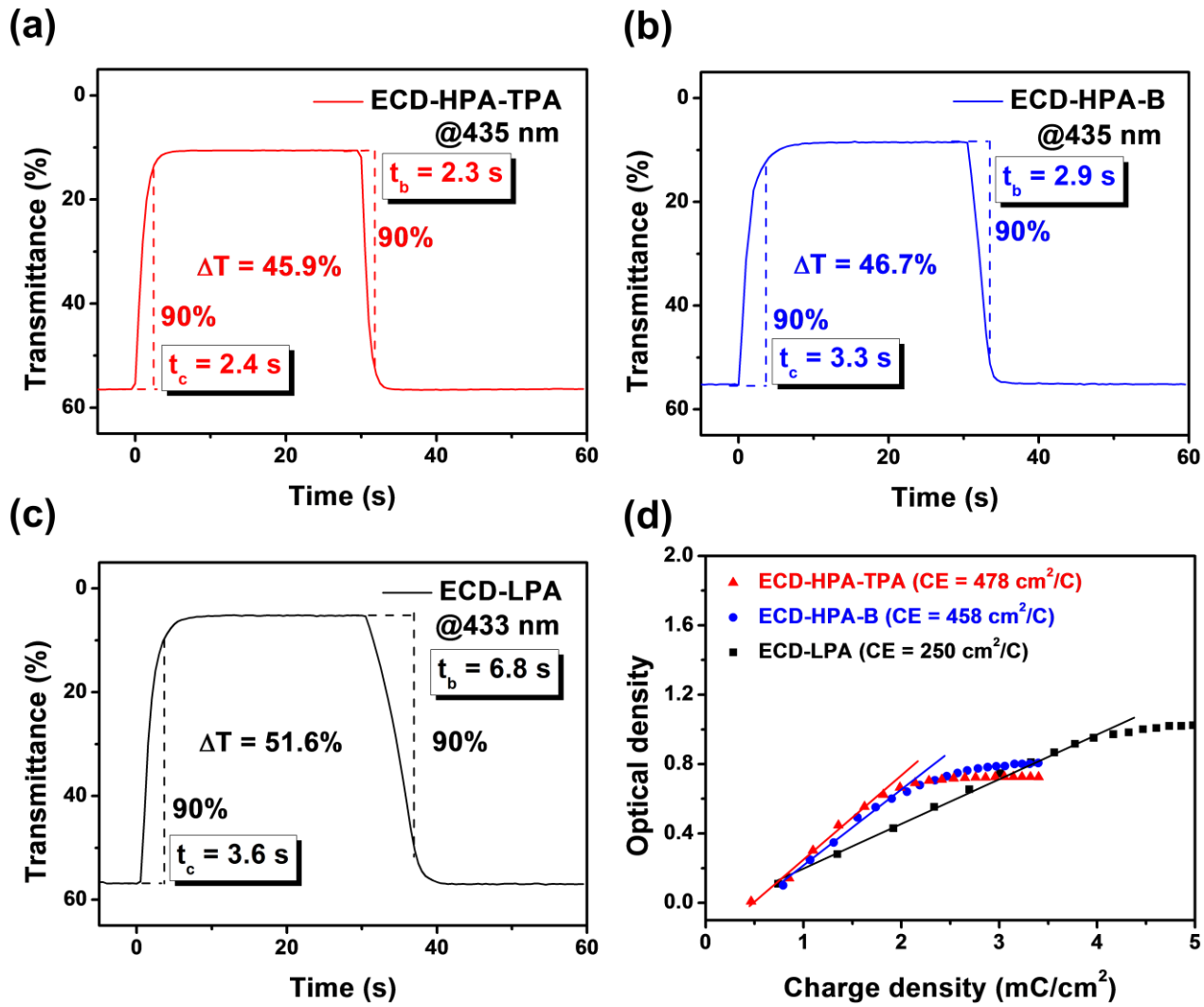

Fig. S30. Response time of (a) **ECD-HPA-TPA** (thickness: 330 ± 30 nm), (b) **ECD-HPA-B** (thickness: 320 ± 20 nm), and (c) **ECD-LPA** (thickness: 350 ± 20 nm) between -0.3 and 1.2 V with a cycle time of 60 s on the ITO-coated glass substrate (coated area: 2 cm × 2 cm) in about 48 μL propylene carbonate with 0.1 M $TBABF_4$ and 0.015 M $HV(BF_4)_2$ as electrolyte. (d) Optical density *vs.* charge density of ECDs in the coloration process to obtain coloration efficiency by the fitting slope.

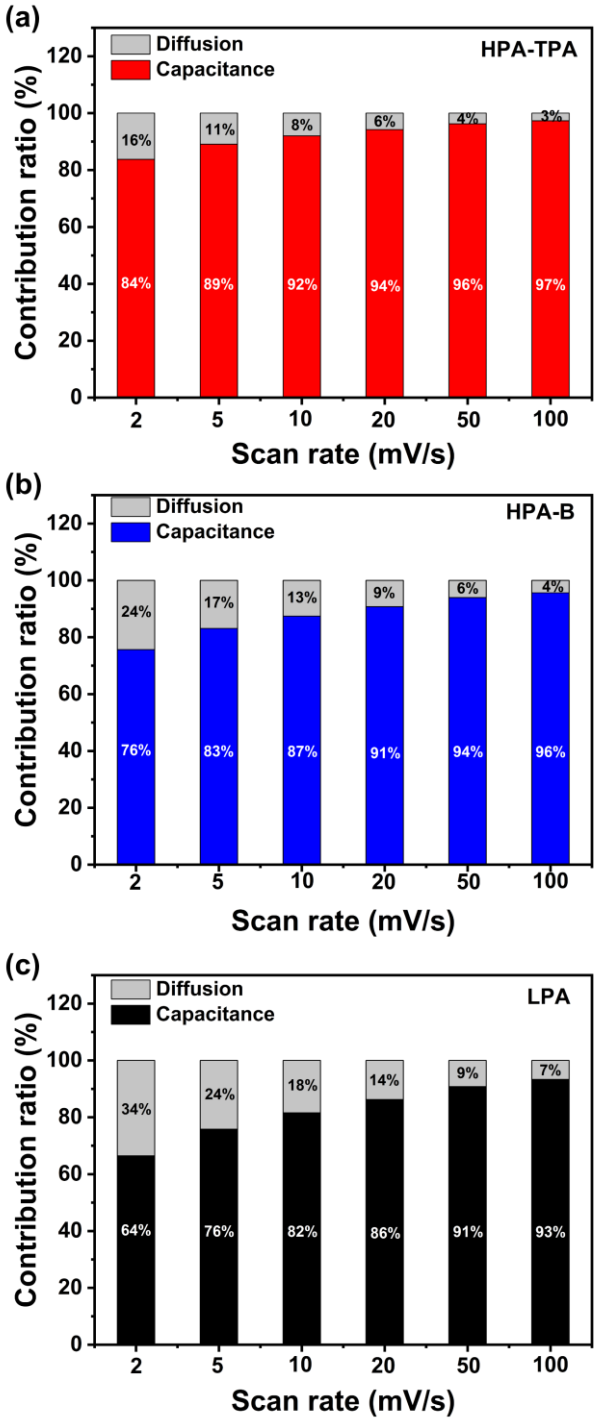

Fig. S31. Comparison of capacitive contribution and diffusion contribution fraction of (a) **HPA-TPA**, (b) **HPA-B**, and (c) **LPA**.

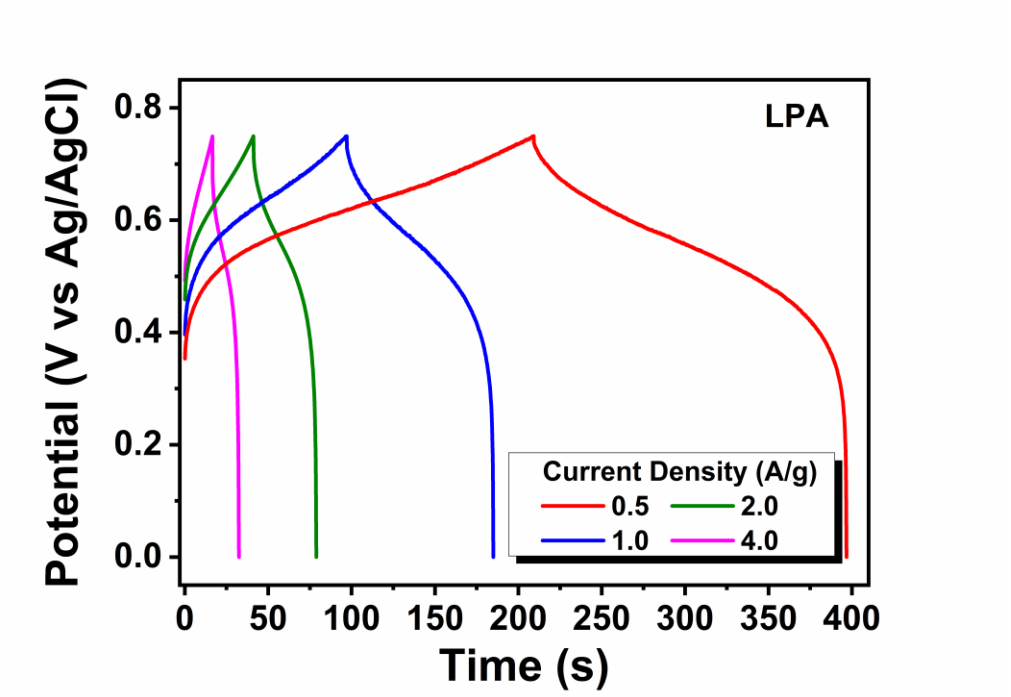

Fig. S32. Galvanostatic charge-discharge diagram of **LPA** at different applied current densities. (thickness: 220 ± 20 nm)

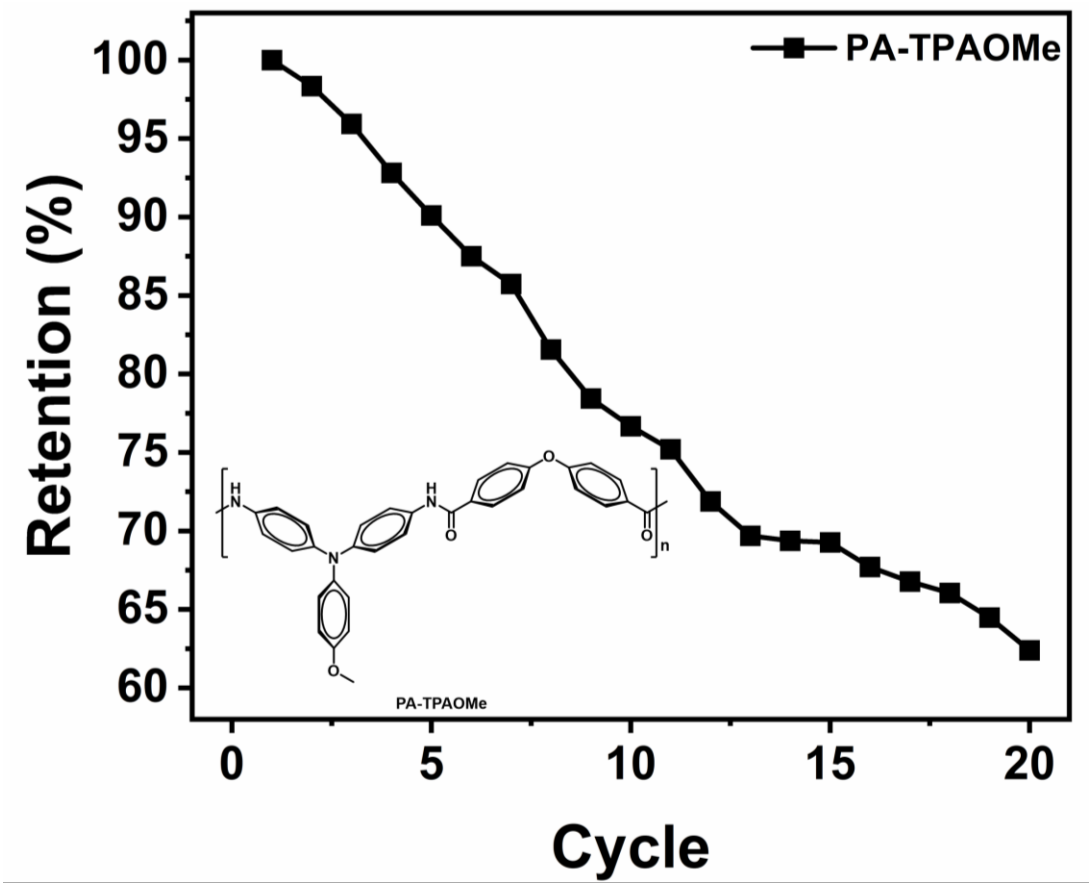

Fig. S33. GCD stability measurements of **PA-TPAOMe** at 1.0 A g^{-1}.

Table S1. Inherent viscosities, molecular weights of polyamides.

Polymers	η_{inh} [a] (dL/g)	M_w [b] (kDa)	M_n [b] (kDa)	PDI [c]
LPA	0.47	44.9	23.1	1.9
HPA-B	0.27	41.6	17.8	2.3
HPA-TPA	0.28	67.2	34.8	1.9

[a] Measured at a concentration of 0.5 g/dL in NMP at 30 °C.

[b] Calibrated with polystyrene standards, using NMP as the eluent with 20 mM LiCl at a constant flow rate of 0.35 mL/min at 40 °C.

[c] Polydispersity index = M_w/M_n.

Table S2. Solubility behaviour of polyamides.

Polymers	Solvents [a]					
	NMP	**DMAc**	**DMF**	**DMSO**	**THF**	**$CHCl_3$**
LPA	++	++	++	++	+−	−
HPA-B	++	++	++	++	+−	−
HPA-TPA	++	++	++	++	+−	+−

[a] Qualitative solubility was tested with 5 mg of a sample in 1 ml of solvent. ++, soluble at room temperature; +, soluble on heat; +−, partially soluble; −, insoluble even on heat.

Table S3. Viscosities and molecular weights of polyamides **HPA-TPA** at different reaction times.

Polymer	Reaction Time (min)	η_{inh} [a] (dL/g)	M_w [b] (kDa)	M_n [b] (kDa)	PDI [c]	DB [d]
HTPA1	30	0.14 (0.25)	20.8	10.3	2.0	0.41
HTPA2	60	0.19 (0.36)	54.0	26.5	2.0	0.48
HTPA3	80	0.24 (0.43)	58.6	28.1	2.1	0.53
HTPA4	100	0.28 (0.47)	67.1	32.6	2.1	0.57

[a] The intrinsic viscosity was calculated and measured at a concentration of 0.5 g/dL in NMP at 30 °C. The values in parentheses are the reduced viscosity, fitted and depicted in **Fig. S16a**.

[b] Used polystyrene as standards, employing NMP as the eluent with 20 mM LiCl at a consistent flow rate of 0.35 mL/min, maintained at 40 °C. [c] Polydispersity index = M_w/M_n.

[d] Degree of branched determined by deconvolution of ^{1}H-NMR spectra.

Table S4. Thermal properties **HPA-TPA**, **HPA-B**, and **LPA** polyamides.

Polymer	T_g [a] (°C)	T_d^5 [b] (°C)		T_d^{10} [b] (°C)		Char yield [c] (%)
		N_2	Air	N_2	Air	
LPA	238	440	430	470	460	65
HPA-B	232	425	400	455	425	61
HPA-TPA	213	435	425	460	460	68

[a] Glass transition temperature, T_g, was measured by DSC 2nd trace with a heating rate of 20 °C/min.

[b] Temperature at weight loss of 5% and 10% polymer recorded by TGA at a heating rate of 20 °C/min and a gas flow rate of 60 cm^3/min. [c] Residual weight percentage at 800 °C in N_2.

Table S5. Results of Nernst equation method.

Polymer	$E_{applied}$ [a] (V)	Fitting equation [b]	n [c]	Electrons [d] (e^-)
HPA-TPA	0.64-0.80	y = 0.0676x + 0.7030	0.87	1
	0.82-0.94	y = 0.0722x +0.8251	0.82	1
	0.98-1.12	y = 0.0768x +0.9674	0.77	1
HPA-B	0.64-0.80	y = 0.0645x + 0.6914	0.91	1
	0.84-1.00	y = 0.0642x +0.8745	0.92	1
LPA	0.50-0.80	y = 0.0765x + 0.6002	0.77	1
	0.86-1.02	y = 0.0708x + 0.9068	0.83	1

[a] Versus Ag/AgCl measured on the ITO-coated glass substrate with 0.1 M $TBABF_4$ in 3 mL MeCN.

[b] Plot $E_{applied}$ vs. $\log(A_n - A_0)/(A_{max} - A_n)$ at the relative wavelength.

[c] Calculated from the slope of the fitting equation and the Nernst equation value of 0.059.

[d] Amount of n electrons transferred for each stage.

Table S6. Electrochromic properties and switching response time of polyamide films.

Polymer [a]	λ_{abs} (nm)	Potential (V)	ΔT [b] (%)	Response time		υ [e] (% s^{-1})	η_{CE} [f] (cm^2 C^{-1})
				t_c [c] (s)	t_b [d] (s)		
LPA	980	0.80	88.8	7.4	2.4	10.8	295
	433		55.7	7.2	3.5	7.0	185
HPA-B	1000		83.2	4.5	2.2	16.6	450
	435		58.9	5.0	3.3	10.6	447
HPA-TPA	1000		84.4	4.3	1.9	17.6	595
	435		58.2	4.4	2.8	11.9	558

[a] The thickness: **LPA** (300 ± 40 nm), **HPA-TPA** (310 ± 40 nm), and **HPA-B** (300 ± 30 nm).

[b] Optical contrast ratio is $\Delta T = T_b - T_c$, where T_b and T_c are transmittances of the bleaching and colouring states, respectively.

[c] Colouring time from the neutral state to 90% of the optical change.

[d] Bleaching time from colouring state to 90% of the optical change.

[e] Response speed is defined as 90% of ΔT divided by t_c.

[f] Colouration efficiency is defined as the slope of the δOD (optical density) *vs.* Q (charge consumed).

Table S7 Electrochemical behaviours of the prepared ECDs.

Polymer [a]	1st oxidation state		2nd oxidation state	
	$E_{oxi.}$ [b] (V)	$E_{red.}$ [c] (V)	$E_{oxi.}$ [b] (V)	$E_{red.}$ [c] (V)
ECD-LPA	1.17	0.93	1.48	1.25
ECD-HPA-B	1.15	0.90	1.48	1.26
ECD-HPA-TPA	1.15	0.94	1.44	1.17

[a] The thickness: **LPA** (350 ± 20 nm), **HPA-B** (320 ± 20 nm), and **HPA-TPA** (330 ± 30 nm) on the ITO-coated glass substrate (coated area: 2 cm x 2 cm) in about 48 µL propylene carbonate with 0.1 M $TBABF_4$ and 0.015 M $HV(BF_4)_2$ as electrolyte.

[b] Oxidation potential at the peak at a scan rate of 50 mV/s.

[c] Reduction potential at the peak at a scan rate of 50 mV/s.

Table S8 Electrochromic properties and switching response time of ECDs**.**

Polymer [a]	λ_{abs} (nm)	Potential (V)	ΔT [b] (%)	Response time		v [e] (% s^{-1})	η_{CE} [f] (cm^2/C)
				t_c [c] (s)	t_b [d] (s)		
ECD-LPA	433	1.2	51.6	3.6	6.8	12.9	250
ECD-HPA-B	435		46.7	3.3	2.9	12.7	458
ECD-HPA-TPA	435		45.9	2.4	2.3	17.2	478

[a] The thickness: **LPA** (250 ± 20 nm), **HPA-B** (270 ± 20 nm), and **HPA-TPA** (260 ± 30 nm) on the ITO-coated glass substrate (coated area: 2 cm x 2 cm) in 0.1 M $TBABF_4$/PC electrolyte with 0.015 M $HV(BF_4)_2$.

[b] Optical contrast ratio is $\Delta T = T_b - T_c$, where T_b and T_c are transmittances of the bleaching and colouring states, respectively.

[c] Colouring time from a neutral state to 90% of optical change.

[d] Bleaching time from colouring state to 90% of the optical change.

[e] Response speed is defined as 90% of ΔT divided by t_c.

[f] Colouration efficiency is defined as the slope of the δOD (optical density) *vs.* Q (charge consumed).

Table S9 Summary of specific capacitance (C_{sp}), energy density (*E*), and power density (*P*).

Current Density [A g^{-1}]	HPA-TPA			LPA		
	C_{sp} [F g^{-1}]	*E* [Wh kg^{-1}] [a]	*P* [W kg^{-1}] [b]	C_{sp} [F g^{-1}]	*E* [Wh kg^{-1}] [a]	*P* [W kg^{-1}] [b]
0.5	**78.9**	**6.2**	**188.8**	**125.1**	**9.8**	**187.5**
1	**73.2**	**5.7**	**373.8**	**117.5**	**9.2**	**376.0**
2	**43.5**	**3.4**	**750.9**	**100.5**	**7.8**	**744.8**
4	**32.0**	**2.5**	**1500.0**	**84.8**	**6.6**	**1494.3**

[a] Energy density (*E*) calculated by $E = \frac{0.5 C_{sp} \Delta V^2}{3.6}$.

[b] Power density (*P*) calculated by $P = \frac{E \times 3600}{\Delta t_{discharge}}$.

Table S10 Comparison table of the different polymeric electrodes in electrochromic supercapacitors.

Material	Polymer Type	Electrolyte	ΔT	η_{CE} [cm^2/C]	Thickness	Specific Capacitance (Current Density)	Reference
PETC	Conjugated Polymer	$LiClO_4$/PC	71%	251	2.5 μm	82.2 F g^{-1} (41.1 mF cm−2) @ 0.01 mA cm^{-2}	4
pCDB-EDOT	Conjugated Polymer	$TBAPF_6$/MeCN	25%	158	*ca.* 129 nm	4.65 mF cm^{-2} (0.05 mA cm^{-2})	5
pTBTCB	Conjugated Polymer	$TBAPF_6$/DCM	41.02%	329.3	*ca.* 200 nm	2.96 mF cm^{-2} (0.05 mA cm^{-2})	6
pQWL	Conjugated Polymer	BMIMOTF/PC	38.25%	491.4	*ca.* 100 nm	1.05 mF cm^{-2} (0.05 mA cm^{-2})	7
CONASH	Coordination Polymer	TBAP/MeCN	27%	66	n. a. [a]	26.38 mF cm^{-2} (0.1 m cm^{-2})	8
PA	Non-conjugated Polymer	$LiClO_4$/MeCN	80.6%	275	*ca.* 210 nm	118 F g^{-1} (0.1 A g^{-1})	9
EPA	Non-conjugated Polymer	$LiClO_4$/MeCN	55.21%	108	n. a. [a]	41 mF cm^{-2} (0.1 m cm^{-2})	10

ESPI	Non-conjugated Polymer	$LiClO_4$/MeCN	69.11%	102	n. a. [a]	38 mF cm^{-2} (0.1 m cm^{-2})	11
TPPA-Me-TB	Non-conjugated Polymer	$TBABF_4$/MeCN	78.4%	345	375 ± 30 nm	165.3 F g^{-1} or 21.02 mF cm^{-2} (1.0 A g^{-1})	12
LPA	Non-conjugated Polymer	$TBABF_4$/MeCN	88.8%	295	300 ± 40 nm [b] /220 ± 20 nm [c]	117.5 F g^{-1} or 7.52 mF cm^{-2} (1.0 A g^{-1})	this work
HPA-TPA	Non-conjugated Polymer	$TBABF_4$/MeCN	84.1%	595	310 ± 40 nm [b] /220 ± 10 nm [c]	73.2 F g^{-1} or 4.68 mF cm^{-2} (1.0 A g^{-1})	this work

[a] Not available. [b] Thickness in the electrochromic measurement. [c] Thickness in the GCD measurement.

Reference

1. G. S. Liou, H. Y. Lin and H. J. Yen, *J. Mater. Chem.*, 2009, **19**, 7666-7673.
2. H. Murata and P. M. Lahti, *The Journal of Organic Chemistry*, 2007, **72**, 4974-4977.
3. Y. Ishida, A. C. Sun, M. Jikei and M.-a. Kakimoto, *Macromolecules*, 2000, **33**, 2832-2838.
4. Y. Zhang, F.-Q. Bai, Y. Xie, M. Zhu, L. Zhao, D. An, D. Xue, E. B. Berda, C. Wang and G. Lu, *Chemical Engineering Journal*, 2022, **450**, 138386.
5. Q. Huang, J. Chen, S. Yan, X. Shao, Y. Dong, J. Liu, W. Li and C. Zhang, *ACS Sustainable Chemistry & Engineering*, 2021, **9**, 13807-13817.
6. M. Shao, D. Ji, Z. Xu, J. Dong, X. Lv, M. Ouyang, Y. Lv, D. S. Wright and C. Zhang, *Journal of Power Sources*, 2023, **581**, 233490.
7. L. Zhang, J. Li, J. Wang, Y. Zhao, Y. Tang, W. Li, M. Ouyang and C. Zhang, *Dyes and Pigments*, 2024, **221**, 111779.
8. B. Cong, Y. Xie, Y. Wu, H. Zhou, C. Chen, X. Zhao and D. Chao, *Chemical Engineering Journal*, 2023, **474**, 145528.
9. C.-P. Constantin, M. Balan-Porcarasu and G. Lisa, *Journal of Energy Chemistry*, 2024, **91**, 433-452.
10. Y. Xie, Y. Zhang, M. Li, R. Huang, X. Liu and D. Chao, *Chemical Engineering Journal*, 2023, **470**, 144099.
11. Y. Xie, J. Chen, M. Zhou and D. Chao, *Dyes and Pigments*, 2023, **212**, 111144.
12. Y.-J. Shao, T.-C. Yen, C.-C. Hu and G.-S. Liou, *Journal of Materials Chemistry A*, 2023, **11**, 1877-1885.